MECHANISTIC AND SUBSTRATE SPECIFICITY STUDIES ON *Burkholderia mallei*

QUORUM SENSING SIGNAL SYNTHESIS ENZYME

by

Aubrey N. Montebello

A thesis

submitted in partial fulfillment

of the requirements for the degree of

Master of Science in Chemistry

Boise State University

August 2014

BOISE STATE UNIVERSITY GRADUATE COLLEGE

DEFENSE COMMITTEE AND FINAL READING APPROVALS

of the thesis submitted by

Aubrey N. Montebello

Thesis Title: Mechanistic and Substrate Specificity Studies on *Burkholderia mallei* Quorum Sensing Signal Synthesis Enzyme

Date of Final Oral Examination: 27 June 2014

The following individuals read and discussed the thesis submitted by student Aubrey N. Montebello, and they evaluated her presentation and response to questions during the final oral examination. They found that the student passed the final oral examination.

Rajesh Nagarajan, Ph.D.   Chair, Supervisory Committee

Don Warner, Ph.D.   Member, Supervisory Committee

Julia Oxford, Ph.D.   Member, Supervisory Committee

The final reading approval of the thesis was granted by Rajesh Nagarajan, Ph.D., Chair of the Supervisory Committee. The thesis was approved for the Graduate College by John R. Pelton, Ph.D., Dean of the Graduate College.

DEDICATION

       I dedicate this work to my supportive and loving friends and family. Their constant encouragement was a blessing during the struggles I have endured through this process. My mother, father, and Nonie were amazingly helpful and relieved a lot of burdens. I will always miss you, Nonie. This is for my husband who was the reassuring force I needed to make it through the early mornings, the long research hours, and the successes and pitfalls involved in research. He was by my side at every moment and I know I couldn't have done it without his support.

ACKNOWLEDGEMENTS

I would like to thank the staff and faculty of the Department of Chemistry at Boise State University for their constant encouragement and dedication to my success. Also, thank you to Ryan Brecht for his HPLC data. I would like to acknowledge my graduate committee members for all of their effort and useful guidance. Dr. Julia Oxford and Dr. Shin Pu were pivotal in successfully identifying substrates. Dr. Don Warner was always available for guidance and helped me to develop a greater understanding of Organic Chemistry. Furthermore, I would like to thank Dr. Rajesh Nagarajan for his time, understanding, wisdom, and dedication that not only helped me academically but mentored me to become a research professional.

ABSTRACT

Gram-negative bacteria use acyl-homoserine lactone (AHL) based quorum sensing (QS) to regulate the expression of genes that give the bacteria a selective advantage over host defenses and antibiotic treatment. *Burkholderia mallei* is an antibiotic resistant pathogen that causes Glanders disease. *B. mallei* BmaI1 AHL-synthase uses octanoyl-Acyl Carrier Protein (C8ACP) and S-adenosyl-L-methionine (SAM) to synthesize the AHL, octanoyl-homoserine lactone (C8HSL). Inhibiting AHL-synthases has been difficult because mechanistic and substrate specificity details for these enzymes are not well understood. Our goal was to determine how BmaI1 activity and enzymatic mechanism changes with nonspecific, variable acyl chain acyl-ACP substrates. We found that catalytic efficiency of nonspecific acyl-ACP substrates are drastically low compared to the native C8ACP substrate, in-line with tight signal specificity observed *in vivo*. In addition, substrates with lower catalytic efficiency also showed kinetic cooperativity while reacting with BmaI1. Our results suggest that substrates add by a preferred order, random sequential mechanism to BmaI1. Alternatively, BmaI1 could exist in two forms, where nonspecific substrates bind to the less active enzyme form and leads to the formation of an unproductive E.acyl-ACP complex. Apparently, only the native acyl-ACP substrate forms both a stable and productive E.acyl-ACP complex, thus providing a molecular basis for substrate discrimination in QS signal synthesis in *B. mallei*.

TABLE OF CONTENTS

LIST OF TABLES

LIST OF FIGURES

LIST OF ABBREVIATIONS

QS	Quorum Sensing
AI	Autoinducer
AIP	Autoinducer Peptide
AI-1	Autoinducer-1
AHL	Acyl-homoserine-lactone
AI-2	Autoinducer-2
AI-3	Autoinducer-3
Apo-ACP	acyl-carrier protein
Acyl-ACP	acyl-acyl-carrier protein
C8ACP	octanoyl-ACP
3-OH-C8-ACP	3-hydroxy-octanoyl-ACP
C6ACP	hexanoyl-ACP
C4ACP	butyryl-ACP
C10ACP	decanoyl-ACP
3-OH-C6-ACP	N-3-hydroxy-hexanoyl-ACP
N-3-OH-C10-ACP	N-3-hydroxy-decanoyl-ACP

SAM	S-adenosyl-L-methionine
ATP	adenosine triphosphate
MTA	methylthioadenosine
HSL	homoserine-lactone
C8HSL	octanoyl-homoserine-lactone
BmaI	*Burkholderia mallei* Initiator
BmaR	*Burkholderia mallei* Receptor
MNCs	Multi-nucleated giant cells
Sfp	Surfactin-synthetase activating protein/phosphopantetheinyl transferase
CoA	Coenzyme A
C8CoA	octanoyl-CoA
C10CoA	decanoyl-CoA
HCl	Hydrochloric acid
UV-Vis	Ultraviolet Visible light
DCPIP	2,6-dichlorophenolindophenol
MES	2-(N-morpholino)ethanesulfonic acid
Tris	Tris(hydroxymethyl)aminomethane
ACC	acetyl-CoA carboxylase

RT   Retention Time

ON   Over night

TCA   trichloroacetic acid

CHAPTER ONE: INTRODUCTION

Quorum Sensing

Quorum sensing (QS) is a type of bacterial intercellular communication that occurs at high cell population densities.[1] QS coordinates bacterial behaviors so as to function like a multicellular organism. The behaviors governed by QS are those that when attempted by individual cells are unproductive, however, when attempted by the masses provide an evolutionary advantage.[2,3] The chemical signal molecules responsible for QS are diffusible, low molecular weight (c. 170-300 Da) pheromones referred to as autoinducers (AIs).[4] QS is achieved through the accumulation of AIs that enable individual cells to sense when the minimal population unit or "quorum" of bacteria has been achieved for a concerted population response to be initiated.[4]

The regulatory components and molecular mechanisms of QS differ among bacterial species. Nonetheless, there are three basic principles that apply to all cases of QS. First, all communicating bacteria produce AIs. When there is a low population within a bacterial community, the AIs synthesized are in such low concentration that they are unable to stimulate a population-wide response. Once a population reaches high density, the cumulative amount of AIs produces a global response. The second principle of QS is that receptors for AIs exist in the membrane or in the cytoplasm of the responding cells. AIs secreted from one cell bind to neighboring bacteria. Lastly, AIs induce the expression of a variety of genes that can stimulate production of additional AIs

through a positive feedback loop to sponsor synchronous behavior in the cell population (Fig. 1).[5]
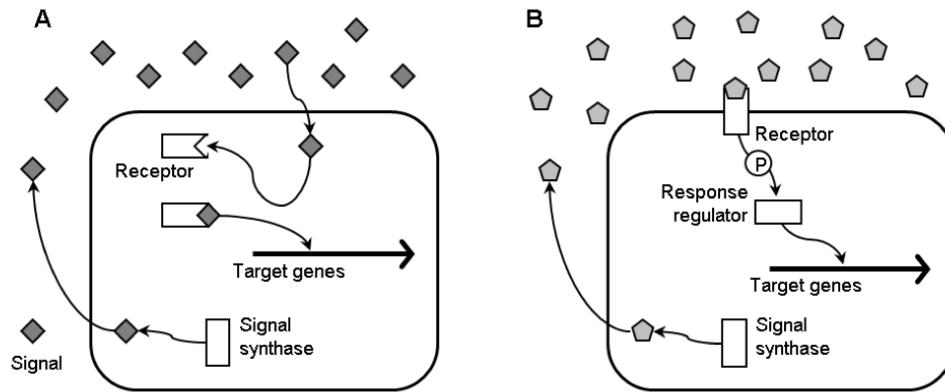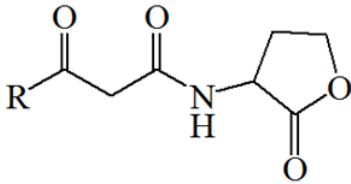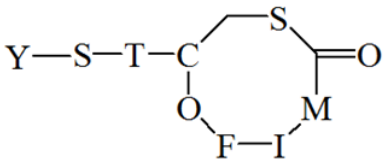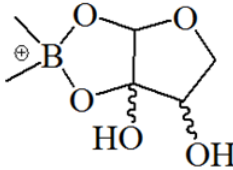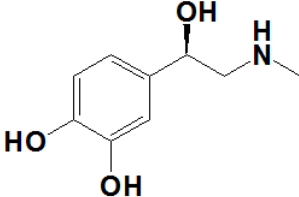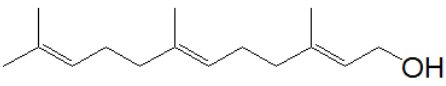
Figure 1.   General scheme of a QS system. The signal synthase enzyme produces signal molecules (AIs), which diffuse or are transported to the extracellular environment. At an optimal concentration of the signal, the AI binds to the receptor, which can be located in the cytoplasm (A) or at the cell surface (B). If the receptor is located in the cytoplasm, the AI-receptor complex activates or inactivates the transcription of target genes. When the receptor is located at the cell surface, the signal induces a phosphorylation signal transduction cascade. This activates a transcriptional regulator that leads to targeted gene transcription.[5]

QS was discovered 30 years ago in two light-producing bacterial species, *Vibrio fisheri* and *Vibrio harveyi*.[1,2] These bacteria emitted light at high cell population density, when the accumulation of secreted AIs stimulated the expression of the structural operon luxCDAB.[6,7] This operon encodes the light producing luciferase enzyme. Today, QS has been observed in both Gram-negative and Gram-positive bacteria though the mechanism of QS differs.

Table 1. **Classification of QS autoinducer molecules**

AI Type	AI Molecule
AI-1 **AHL**	
AIP	
AI-2 **Universal**	
AI-3	
Farnesol	

Gram-positive bacteria use small cyclic peptides called autoinducer peptides (AIP) as signaling molecules (Table 1).[3,7] The AIPs are synthesized in the cytoplasm and are actively transported out of the cell to interact with a two-component type extracellular domain of membrane bound sensor receptors.[6,7] The bound AIP initiates a phosphorylation cascade that modulates the activity of a DNA-binding protein that regulates transcription of target genes. This protein is termed a response regulator and is highly selective for a given peptide signal.[3,6,7] This selectivity allows the bacterial

community to communicate efficiently. Gram-positive bacteria can use multiple AIs and receptors in series or in parallel to achieve desired behaviors. One Gram-positive bacteria, *Staphylococcus aureus*, synthesize AIPs to regulate the *agr* system that controls more than 70 genes that are known to code for virulence factors.[8]

Quorum sensing in Gram-negative bacteria does not involve the use of AIPs. In Gram-negative bacteria, small molecules known as acyl-homoserine-lactones (AHL/AI-1) are used as QS signaling molecules (Table 1). QS in the *V. fischeri sp.* is the most extensively studied system to date.[9-12] Two regulatory proteins, LuxI and LuxR, are responsible for biosynthesis of the AI and subsequent behavior of the bacteria. The AHL diffuses across cell membranes and, at optimal concentrations, binds to the LuxR receptor, which regulates the transcription of a multitude of genes. The Gram-negative bacterium *Pseudomonas aeruginosa* produces two AHL signals to regulate more than 350 genes that regulate extracellular virulence factors, biofilm formation, and antibiotic efflux pumps.[13-15]

In addition to the AIP and AI-1 systems, a universal signal molecule that allows inter-species communication has also been observed.[3,16] This signal molecule is AI-2 (Table 1). When AI-2 is bound to its receptor, a phosphorylation signal cascade is initiated that influences the activity of a DNA-binding transcription protein.

Although AI-1, AI-2, and AIP signaling systems have been extensively studied, other AI QS systems are known. These include the epinephrine-like AI structure (AI-3) observed in *E. coli* O157:H7 that appears to regulate the formation of lesions as well as the isoprenoid farnesol AI signal found in the yeast *Candida albicans* (Table 1).[16-18] The interest of the work herein concerns gram negative QS systems. Many of the genes

transcribed by the QS molecules listed in Table 1 are those that lead to virulence, which includes toxin release, biofilm formation, and resistance.

Biofilms and Resistance

Biofilms allow bacteria to exist within a community rather than being singly dispersed in an environment. Communal existence is optimal for survival and therefore the majority of bacteria in nature are found within biofilms. Biofilms can have one species of bacteria or be a multi-species biofilm. Biofilms provide a safe environment for survival and symbiotic relationships so that optimal microenvironments exist.[19,20]

Biofilm formation occurs when planktonic bacterial cells adhere to a surface and an optimal cell density is reached so that AI molecules signal QS. The QS signaling pathways lead to altered gene transcription to produce an exopolysaccharide matrix.[21] This matrix envelops the micro-colony. Inside the micro-colony, further alteration of genes produce a wide array of behaviors and phenotypes including attaining communal existence of an individual bacterial cell and up-regulation of genes encoding enzymes, transporters, and channels.[19,22,23] The regulation of these genes produces a toxic and hazardous environment for foreign invaders.

Biofilms are composed of a collection of bacterial cells that secrete the polysaccharide matrix. This thick, sticky matrix acts as a shield against the host's immune response by preventing access to the entire micro-colony. Its depth limits both phagocytosis by neutrophils and antibiotics intervention by preventing full eradication of all the microbes in the community.[24] Therefore, biofilms allow bacteria to become resistant to the host's immune defense as well as pharmacological intervention. Over

80% of bacterial infections in humans involve the formation of a biofilm.[25,26] This has led to research into targeting QS when developing therapeutics.

Quorum Sensing as a Drug Target

Multi-drug resistant bacteria pose major hurdles for antibacterial therapy. The ability of bacteria to resist antibiotic treatment was first observed in the late 1930s-1950s after the widespread dispersal of sulfonamides and penicillin.[24,25] The majority of antibacterial compounds work by killing the bacteria as a whole. Mutations in bacteria as well as improper use of drugs allow the species to survive and adapt to subsequent treatments, ideally becoming multi-drug resistant. Today, bacteria have the ability to gain resistance to every antibiotic used in treating infections. Therefore, there is a need to prevent multi-drug resistance from occurring when treating bacterial infections. One such option is to target the QS system used by the bacteria. This would not kill the bacteria as a whole, but would prevent the transcription of genes that lead to biofilms and resistance. The host's immune response should be able to then actively target the infection and successfully kill the bacteria. This approach is advantageous over conventional antimicrobial agents because (1) the likelihood for rapid mutations to occur that develop drug resistance is low; (2) beneficial normal flora of the host is not killed; (3) not immediately killing the bacteria may allow the host to mount a robust immune response and therefore eliminate the infection without the need of bactericidal agents; and (4) not immediately killing the bacteria would prevent the massive release of toxic lipopolysaccharides associated with bacterial death, which often leads to sepsis.[26]

Figure 2. **AHL-synthase substrate, AHL signal and bacterial phenotype.** Over 70 gram negative bacterial species have been discovered to produce AHL. AHL lead to phenotypic behavior that is virulent to the host.

Quorum sensing can be inhibited at one or more steps in QS pathways. In Gram-negative bacteria, the initiator and receptor proteins (LuxI/LuxR type) are targets for inhibition. One option that has been explored is to design receptor inhibitors/antagonists, which can bind to the AHL receptor but not elicit the subsequent biological response.[26-28] Blackwell and coworkers have reported a number of AHL receptor antagonists that showed biofilm inhibition activity.[26-29] Most of these antagonists are designed as modified AHLs. The modifications include acyl chain and/or the lactone ring variations in the native AHL AI. Since multiple receptors are used to control QS in a cell, targeting the receptor to inhibit QS is very difficult. In addition, AHL receptors bind to their cognate AI with nanomolar affinities and therefore it is difficult to design ligands that could outcompete these tight-binding native AHLs. Another option is to inhibit the initiator protein to stop the AI from being generated at sufficient levels required for

intercellular communication. This approach can prevent the biofilm from forming because synthesis of the AHL signal would be insufficient to initiate a QS signal cascade. In fact, studies involving *P. aeruginosa* null mutants that lack the LasI AHL synthase show a decrease in biofilm formation and attenuated virulence.[30] Although inhibition of AHL synthesis is desirable to interrupt interbacterial communication, designing AHL-synthase inhibitors are not straightforward because the mechanism of AHL synthesis is poorly understood. *A key objective of this thesis is to address mechanistic questions on Burkhloderia mallei BmaI1 AHL-synthase enzyme*. We believe that a deeper understanding of the mechanism of AHL synthesis will accelerate the discovery of QS inhibitors.

AHL-synthase; BmaI1

In Gram-negative bacteria, the AHL-synthase enzyme responsible for making AHL AI signal are most often members of the LuxI protein family and have sequence similarity.[30] There have been over 70 different AHL-synthases discovered to date that produce specific AHL signal molecules (Fig. 2). These bacteria are pathogens to humans, animals, plants, aquatic life, and more due to the LuxI/LuxR QS system. Some examples of AHL-synthases known that lead to virulence factor expression include V. *fisheri* LuxI AHL-synthase (aquatic pathogen), *Agrobacterium tumefaciens* TraI AHL-synthase (aquatic and human pathogen), *Pantoea stewartii* EsaI AHL-synthase (plant pathogen), *Pseudomonas aeruginosa* LasI and RhlI AHL-synthase (human pathogen), and the *Burkholderia mallei* BmaI1 AHL-synthase (animal and human pathogen). The focus of this thesis is to address mechanistic questions on an AHL-synthase protein from *B. mallei*, BmaI1.

B. mallei was first isolated by William Schutz and Friedrich Loffler in 1882.[31,32] B. *mallei* is an opportunistic, aerobic, animal, and human pathogen found in the air and water. *B. mallei* infects by lysing entry vacuoles in the host's cell. It gains motility once inside the cell and can escape from cells during immune responses and antibacterial defenses through use of multi-nucleated giant cells (MNCs).[31] This motility and evasion process lets the bacteria survive in the host longer, eventually forming a micro-colony and becoming virulent to the host.

Glanders disease results from a *B. mallei* infection. Glanders is primarily a disease affecting horses, but it also affects donkeys, mules, goats, dogs, cats, and humans.[31] Geographically, the disease is found in Africa, Asia, the Middle East, and Central and South America. Animal infections are common in these areas, but human infections have only occurred rarely and sporadically. Most human infections occurred in laboratory workers and those in direct and prolonged contact with infected, domestic animals. This bacterium has shown resistance to a number of antibiotics including aminoglycosides, polymyxins, and beta-lactams. [31,32]

Even though there is wide spread knowledge of *B. mallei* infections that result in Glanders disease, there is little known about the enzymes responsible for the AHL signaling. There are multiple BmaI-BmaR QS systems responsible for virulence found in *B. mallei* including BmaI1-BmaR1, BmaI3-BmaR3, and the LuxR orphan proteins BmaR4 and BmaR5. These systems use different acyl-ACPs to produce AHLs for a QS response including octanoyl-ACP (C8ACP), 3-hydroxy-octanoyl-ACP (3-OH-C8-ACP), hexanoyl-ACP (C6ACP), N-3-hydroxy-hexanoyl-ACP (3-OH-C6-ACP), and N-3-hydroxy-decanoyl-ACP (N-3-OH-C10-ACP.[32,33] Because pathogenic bacteria like *B.*

mallei use AHL signals to regulate virulence genes, an understanding of the mechanism

of signal synthesis may lead to the development of QS-targeted anti-virulence molecules.

AHL-synthase Proposed Mechanism

AHLs are derived from S-adenosyl-L-methionine (SAM) and acyl-acyl-carrier

protein (acyl-ACP). The enzymes responsible for synthesizing AHLs are LuxI family

AHL-synthases.[36,37] The proposed mechanism for synthesizing all AHLs (Fig. 3) suggests

that a general base in the AHL-synthase active site deprotonates the SAM-amine. The

nucleophilic SAM-amine attacks the carbonyl center on the acyl-ACP releasing holo-

ACP. Lactonization of the SAM intermediate produces the AHL and

methylthioadenosine (MTA). BmaI1's native acyl-ACP substrate is octanoyl-ACP

(C8ACP). When combined with SAM and C8ACP, this enzyme produces the QS AI

signal octanoyl-homoserine-lactone (C8HSL).[33] BmaI1 is auto-regulated by the C8HSL

signal and the BmaR1 receptor.
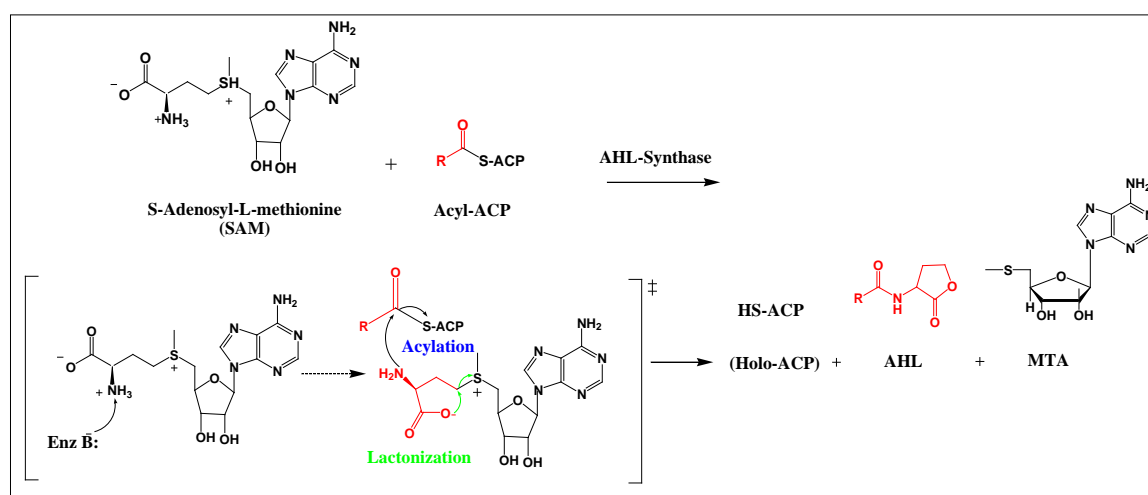
Figure 3.   **Proposed mechanism for AHL-synthase.** The acyl-ACP chain length varies for each AHL-synthase. For the AHL-synthase BmaI1, octanoyl-ACP (C8ACP) is the substrate and octanoyl-HSL (C8HSL) is the AHL signal.

AHL-synthase Substrates

S-Adenosyl-L-Methionine (SAM)

   SAM is synthesized in the cytosol by methionine adenosyl-transferase, which joins L-methionine to ATP and yields SAM, pyrophosphate, and phosphate ion.[33]   SAM is primarily a methyl group donor in methylation reactions of macromolecules and small molecules. It is uniquely used with AHL-synthases not as a methyl donor but to form a lactone ring in AHL product.

   SAM is commercially available and frequently used when studying AHL-synthases. Commercially available samples of SAM formulations are most stable at acidic pH and at lower temperatures.[34] The purity of SAM varies due to the degradation of SAM by cleavage into MTA and HSL and hydrolysis to adenine and S-(5`-deoxyribosyl)-L-methionine. The products of this degradation are also products in the AHL-synthase reaction (Fig. 4).[34]
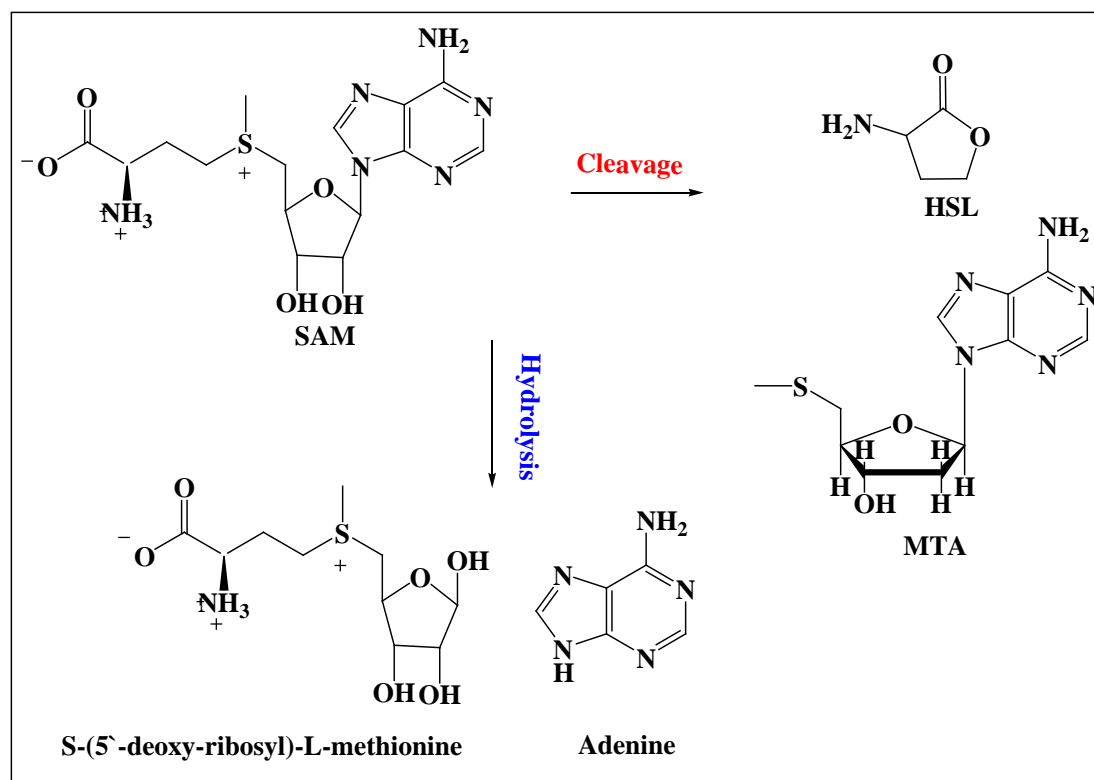
Figure 4. **Chemical degradation products of SAM.** HSL and MTA are products of AHL-synthase and can inhibit the reaction.[34]

To improve SAM stability, commercially available formulations with larger molecular weight salts were prepared. It is unknown whether these SAM-salts affect AHL-synthase activity. SAM-salts formulations like SAM-Cl, SAM-I, and SAM-tosylate have various sized anionic salts that potentially can affect the activity of AHL-synthases. *One objective of this work is to study how different formulations affect SAM substrate activity with AHL-synthase*.

Acyl-Acyl Carrier Protein (Acyl-ACP)

One reason AHL-synthases are difficult to study kinetically is because acyl-ACPs are not commercially available. These substrates are synthesized within the bacterial cell during type 2 fatty acid biosynthesis. There are two laboratory methods for preparing acyl-ACPs; a chemical and enzymatic method.[35]

In the chemical method for synthesizing BmaI1's substrate octanoyl-ACP, an *activated* octanoic acid is coupled with holo-ACP to make octanoyl-ACP. Cronan has shown that fatty acid acyl-ACP's can be prepared by chemical coupling of N-acyl imidazole (an activated carboxylic acid) with holo-ACP in nearly quantitative yields (Fig. 5).[35]
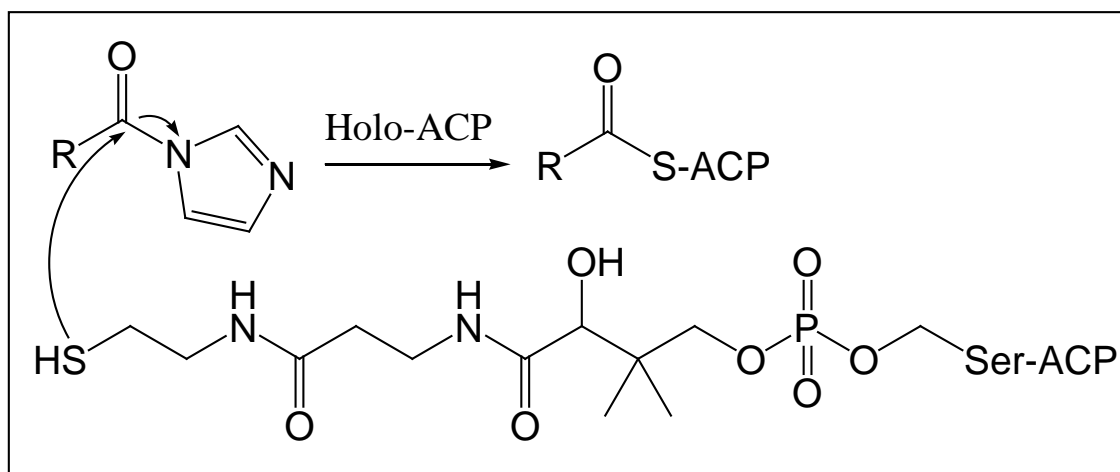
Figure 5. **Chemical synthesis of acyl-ACPs**. An acylated carboxylic acid is activated with the addition of imidazole. Imidazole is a good leaving group and the carbonyl from the activated acid can be attacked by the nucleophilic thiol in holo-ACP.

In the enzymatic method, the enzyme Sfp from *Bacillus subtilis* (a phosphopantetheinyl transferase) converts acyl-CoA to acyl-ACP (Fig. 6).[35] The pantethiene linker and acyl chain in the acyl-ACP is provided from the acyl-CoA. The broad substrate specificity of Sfp enzyme is especially convenient in making several acyl-ACPs from their corresponding acyl-CoAs using this method.
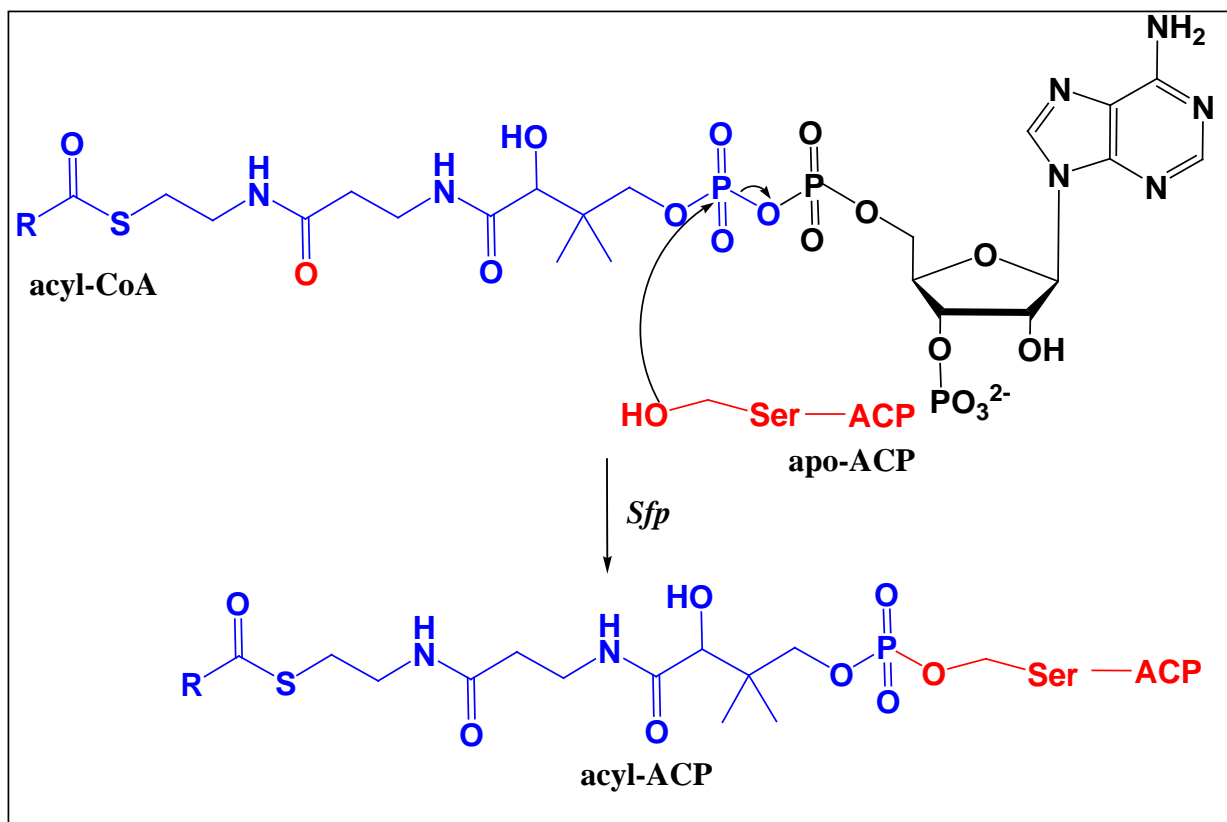
Figure 6. **Enzymatic preparation of acyl-ACP.** Acyl-CoA couples with apo-ACP by nucleophilic attack of the serine hydroxyl of apo-ACP on the phosphate bond shown. The phosphopantethein transferase, Sfp, is the enzyme that aids this conversion.

Several methods have been reported in the literature for purifying apo-ACP and acyl-ACPs. Among them, research groups have routinely precipitated and resuspended the protein. Literature suggests that the purification of apo-ACP from *E. coli* DK547 is optimal when precipitating the lysate with trichloroacetic acid and sodium deoxycholate, and that acyl-ACP can be successfully purified by precipitation in acetone and re-suspendion in a Tris-HCl buffer.[13,36,37] However, to the best of our knowledge, there has been no systematic study on how precipitation and resuspension affects ACP activity. When performing enzymatic studies using acyl-ACP substrates, it is necessary to obtain the native and therefore most active substrate. *An objective of this work is to determine*

how precipitation and resuspendion of apo-ACP and acyl-ACP affects AHL-synthase

activity.

AHL-synthase Assay: DCPIP Assay

Tipton and coworkers reported a colorimetric assay that measured the activity of the AHL-synthase RhlI.[13] This colorimetric assay utilized UV-Vis spectroscopy and the chemical known as 2,6-dichlorophenolindophenol (DCPIP). DCPIP is an oxidizing agent that absorbs at 600 nm. Specifically, DCPIP reduces free thiols. One product of all AHL-synthase reactions is holo-ACP. Holo-ACP contains a free thiol that can be oxidized by DCPIP (Fig. 7). There are two reduction sites for DCPIP, so for every 2 molecules of holo-ACP produced, one molecule of DCPIP is reduced. The concentration of thiol released as a function of time can be measured by following the dye reduction reaction at 600 nm. This method was optimized at pH 7.2 in MES buffer for BmaI1 and was utilized when measuring kinetic constants.
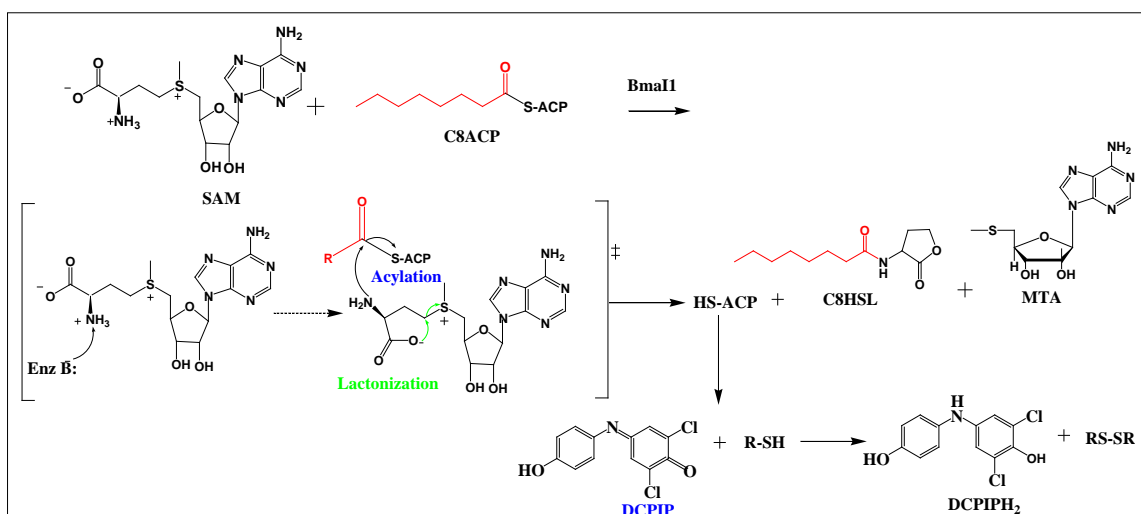
Figure 7.   Proposed mechanism for BmaI1 with DCPIP. DCPIP absorbs at 600 nm. Two molecules of holo-ACP reduce one molecule of DCPIP. The concentration of holo-ACP released can be measured as a function of time. This work studied alternative substrates along with native substrates for BmaI1 using this assay.

AHL-synthase Structure Studies

As mentioned previously, the crystallization of a AHL-synthase bound to substrate have not been successful. Therefore, information concerning substrate active site binding is limited. However, two apo AHL-synthase ribbon structures, EsaI and LasI, have suggested conserved regions of substrate binding sites for all AHL-synthases (Fig. 8).[38-40] The ribbon structures for these enzymes share similarities in binding sites for the acyl chain in acyl-ACP, the ACP, and SAM. The overall structure for these enzymes is a three-layer alpha-beta-alpha sandwich consisting of 8 helices and 9 twisted beta-sheets. These structures closely resemble the acyl-CoA-N-acyl-transferase fold family of proteins.[38]

The ACP binding site was hypothesized from mutagenesis, reporter assays, and structural comparison studies. Acyl carrier protein (apo-ACP) is a 9 kD protein used in fatty acid biosynthesis as a way of transferring hydrophobic fatty acid chains to enzymatic domains so to synthesize phospholipids and other specialized products, including lipid A, lipoic acid, and AHLs.[41-43] Apo-ACP has a conserved four-helix bundle. The fatty acid chain covalently attaches to the phosphopantetheine prosthetic group at the N-terminal end of the helix II in apo-ACP and is located within the hydrophobic interior of this bundle. Computational, crystallographic, and mutagenic studies implicate the acidic central helix II as a "recognition helix" for interaction with most of the ACP enzyme partners.[44] Enzyme-ACP interactions are predominantly electrostatic. Since the recognition helix (helix II) in ACP is negatively charged, a region of the AHL-synthase should have overall positive charge to electrostatically interact. In fact, there are basic residues along alpha-7 and beta-8 in AHL-synthases that form a

positively charged patch on the surface (see Fig. 8 for description of amino acids involved in ACP binding). The flexible loop in LasI and an additional helix close to SAM binding site in EsaI also aid in ACP binding to the enzyme. Both of these regions are suggested to be involved in binding of the holo-ACP portion of acyl-ACP substrate in this enzyme.
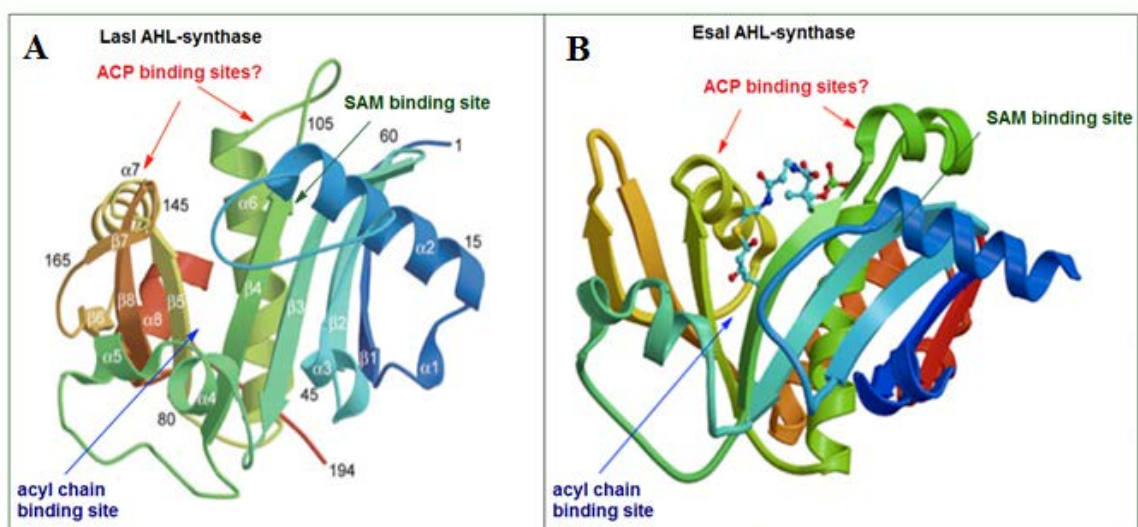
Figure 8.   Ribbon Structures for AHL-synthase. (A) LasI AHL-synthase indicating substrate binding sites. ACP binding site for LasI involve residues including Lys150, Arg154, Arg161, His165, Lys167, and Arg172. Acyl-chain binding pocket resides in the V-cleft and contains the residues Trp33, Trp69, Met79, leu102, Leu122, Met125, Leu140, Thr142, Thre144, Val148, Met151, Met152, Ala155, Leu157, Ile178, and Leu188; specific for LasI. (B) EsaI AHL synthase ribbon structure with 3-oxo-hexanoyl-ACP bound in V-cleft. [38-40]

The acyl chain binding site in AHL-synthase is a V-shaped deep cleft (beta-4 and beta-5 in LasI structure shown) comprised of mostly hydrophobic residues (see Fig. 8 for description of hydrophobic residues in LasI). This hydrophobic domain accommodates the acyl side chain in the active site.[38-40] For LasI, the V-cleft extends deeply because the natural substrate, 3-oxo-dodecanoyl-HSL, has a long acyl-chain. The acyl-ACP in EsaI is 3-oxo-hexanoyl-ACP. In this enzyme, the V-cleft is filled with hydrophobic residues

that narrow the depth to fit the shorter acyl-chain. From these two ribbon structures, it is hypothesized that the V-cleft is modulated according to the acyl-ACP chain length.

An important question to consider is whether alternative acyl-ACPs fit in the V-cleft and turn over. Ideally, the V-cleft for LasI could fit acyl chains varying from twelve to two carbons in position. Likewise, the V-cleft of EsaI could fit acyl chain lengths varying from six to two carbons. Interestingly, it has also been shown that RhlI can make hexanoyl-HSL (C6HSL), which is two carbons longer than the native butyryl-HSL (C4HSL). This indicates that the V-cleft in the active site can accommodate different substrates. The native acyl-ACP for BmaI1 is C8ACP. The work described in this thesis explores whether the V-cleft in BmaI1 can turn over shorter or longer acyl chains. *I hypothesize that studying alternative substrates with BmaI1 can provide clues into AHL-synthase's selectivity for the native substrate.*

AHL Signal Specificity in Gram-negative Bacteria

Bacterial acyl-ACPs are synthesized *in vivo* via type II fatty acid biosynthesis (Fig. 9). This process begins when acetyl-CoA is converted to malonyl-CoA by the enzyme acetyl-CoA carboxylase (ACC). Then, malonoyl-CoA couples with malonyl-CoA:ACP transferase (FabD) to produce malonyl-ACP. Malonyl-ACP combines with acyl-ACP using 3-ketoacyl-ACP synthase (FabB). This produces 3-ketoacyl-ACP. From here, a series of reductions, oxidations, and eperimizations produces the elongated acyl-ACP. Further elongation can continue as the acyl-ACP combines with more malonyl-ACP. These acyl-ACPs can be made into phospholipids, lipid A, lipoic acid, and AHLs.
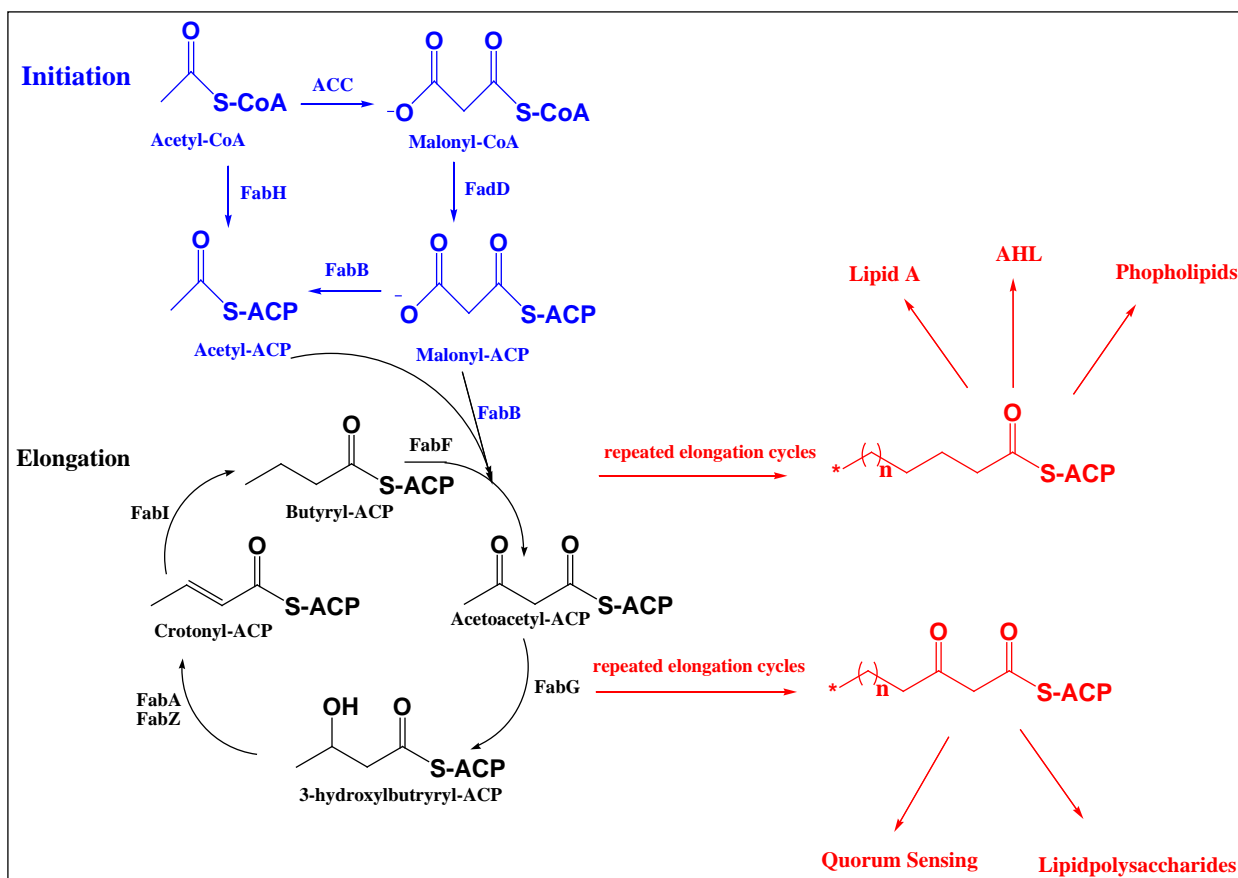
Figure 9. **Type II fatty acid biosynthesis**. Continued elongation cycles produce a large cellular pool of acyl-ACPs.

AHL-synthase specificity ensures the correct AHL signal is produced. During type II fatty acid biosynthesis, there are multiple acyl-ACPs in the cytosol. Hoang *et al*. have shown that if β-ketoacyl ACP reductase (FabG) in fatty acid biosynthesis pathway is rate limiting, LasI synthesized increased amounts of short chain 3-oxo-AHLs both *in vitro* and *in vivo*.[43] This suggests that AHL-synthases can make nonspecific AHL if conditions are limiting.[45] However, mass spectrometry and HPLC studies of AHL-synthases reveal one predominate AHL in each bacterial species.[45] *This means that AHL-synthase must react with one acyl-ACP substrate to produce one AHL signal*. If the right acyl-ACP were not chosen, then AHL-synthases would make multiple AHLs and some of them could be inhibitory to QS. This would result in increased noise in bacterial

signaling that waste cellular energy resources and lead to an inefficient signaling system in bacteria.

The mechanism of tight signal specificity in generation of QS signal is an unsolved mystery. One possible scenario is that fatty acid biosynthesis is regulated to selectively produce the desired acyl-ACP substrate. However, since fatty acid biosynthesis is interconnected to multiple metabolic pathways, it is unlikely to serve as major regulatory point to control QS signal selectivity. An alternative scenario is that AHL-synthase enzymes effectively discriminate between native and nonspecific acyl-ACP substrates. If this is true, AHL-synthase enzymes must be able to discriminate between native acyl-ACP and nonspecific acyl-ACP substrates at one or more of the following steps: *viz.*, binding, catalysis and/or product release (Fig. 10). If a nonspecific substrate binds to AHL-synthase, the enzyme should somehow keep reaction rates with such substrates low enough so that nonspecific signals do not accumulate in the environment. How the enzyme distinguishes between native and nonspecific acyl-ACP substrate is not well understood. *Another key objective of this thesis is to understand how BmaI1 recognizes its cognate C8ACP from shorter and longer chain noncognate acyl-ACPs.*
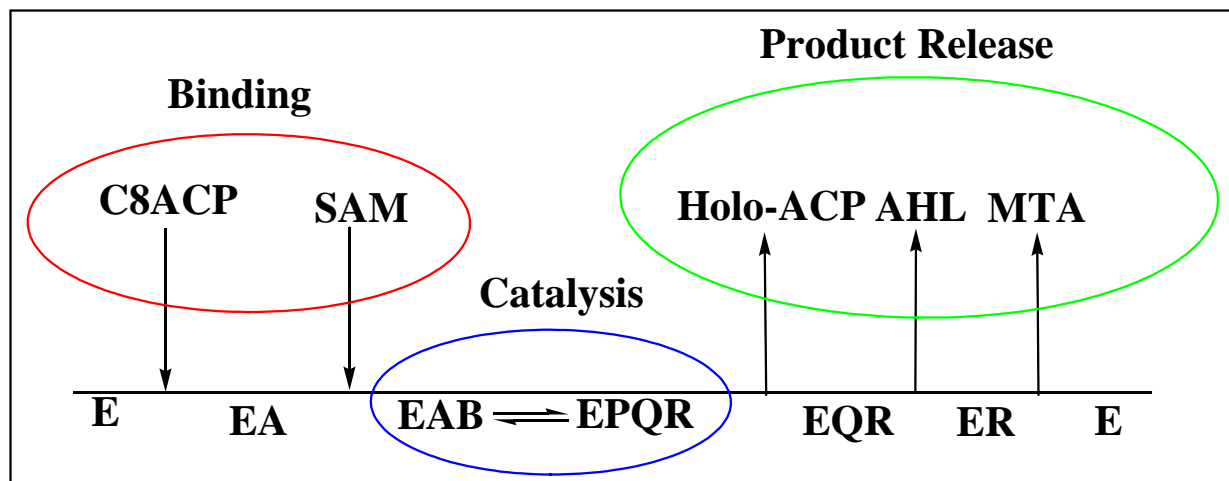
Figure 10. **Enzymatic scheme for a bi-ter ordered mechanism.** Selectivity for substrates can occur at the *viz.*, binding, catalysis or product release steps indicated.

AHL-synthase Kinetic Mechanism

AHL-synthase follows a bi-ter mechanism (2 substrates, 3 products). The order of substrates addition and product release is referred to as the kinetic mechanism. Substrates add to the enzyme through one of the three possibilities: a) the substrates sequentially add in an obligatory order, b) the substrates add sequentially in a random fashion, or c) the substrates add via ping-pong mechanism where the first product is released before the second substrate adds to the enzyme (Fig. 11). The following rules are followed while representing a kinetic mechanism. Enzyme forms are named beginning with 'E'. Substrates are named A (first substrate to bind), B (second substrate to bind), C (third substrate to bind) while products are named P (first product released), Q (second product released), R (third product released) etc. For the RhlI enzyme, substrates add in a sequential manner with SAM substrate binding first to the enzyme and MTA being the last product to be released from the enzyme active site.[13,41,46] However, it is not clear whether all AHL-synthase enzymes follow this mechanism and so it is important to determine the order of substrate binding and product release for the BmaI1 enzyme.
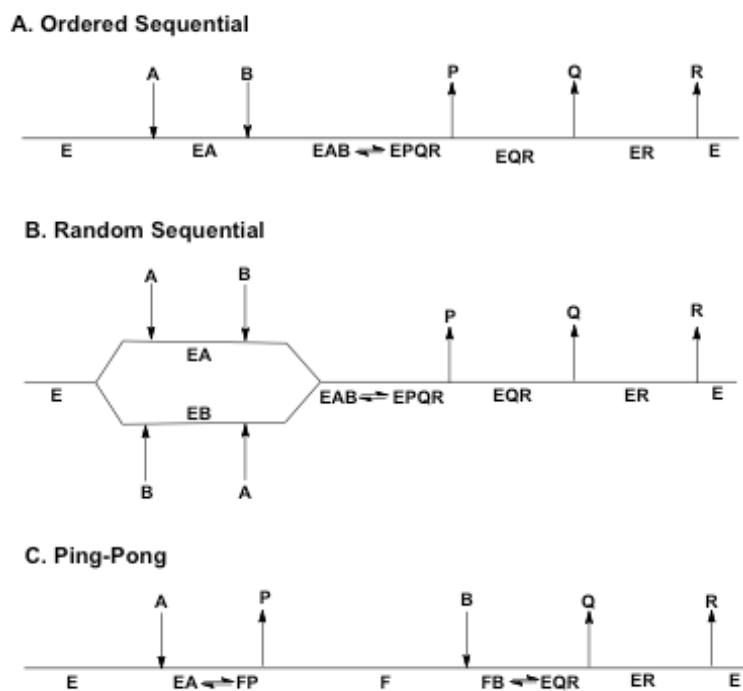
Figure 11.   Kinetic mechanism for bi-substrate enzyme mechanism. (A) Substrates sequentially add in an obligatory order, (B) Substrates add sequentially in a random fashion, (C) Substrates add via ping-pong mechanism where the first product is released before the second substrate adds to the enzyme.

Initial rates for bi-substrate enzymes displaying sequential mechanism (both ordered and random) as a function of substrate concentration is given by the Cleland equation below:

$$V_0 = \frac{V_{\max ab}}{K_i^A K_m^B + K_m^B a + K_m^A b + ab}$$ Equation 1

Here $K_m^{\ A}$ is the Michaelis constant for A at saturating concentrations of B

$K_m^{\ B}$ is the Michaelis constant for B at saturating concentrations of A

$K_i^{\ A}$ is the dissociation constant for EA complex.

For the ping-pong mechanism, the $K_i^A K_m^B$ term in the denominator drops out in Equation 1. Equation 2 is representative of the initial rate for a bi-substrate enzyme displaying a ping-pong mechanism.

$$V_0 = \frac{V_{max}\ ab}{K_m^B a + K_m^A b + ab}$$

Equation 2

These equations can be simplified into a simple Michaelis-Menten (data is interpreted using Michaelis-Menten kinetics) form when one of the substrate's concentrations is held constant. For instance, if Equation 1 has substrate 'b' at a fixed concentration and substrate 'a' at variable concentrations, then the equation reduces to the following Michaelis-Menten form used to describe a single-substrate enzyme reaction:

$$V_0 = \frac{V_{Max}\ [a]}{K_m + [a]}$$

Equation 3

The double reciprocal of Equation 3 will adjust the equation to a linear form (y = mx + b).

$$\frac{1}{V_0} = \frac{K_m}{V_{max}[a]} + \frac{1}{V_{max}}$$

Equation 4

Equation 4 determines the terms for slope and intercept for single substrate kinetics

$$Slope = \frac{K_m}{V_{max}}$$

$$Intercept = \frac{1}{V_{max}}$$

Experimental results are commonly represented in double reciprocal plots. Generated from Equation 1, the double reciprocal plot for a bi-substrate enzyme will have the linear form:

$$\frac{1}{V_0} = \frac{1}{V_{max}} \left[\left(1 + \frac{K_m^B}{b} \right) + \frac{1}{a} \left(K_m^A + K_i^A \cdot \frac{K_m^B}{b} \right) \right]$$

Equation 5

A double reciprocal plot generated from Equation 2 will have the linear form:

$$\frac{1}{V_0} = \frac{1}{V_{max}} \left[\left(1 + \frac{K_m^B}{b} \right) + \frac{1}{a} \left(K_m^A \right) \right]$$

Equation 6

The slope and intercept for random and ordered sequential mechanism at fixed concentration of 'b', using Equation 4 are described below.

$$Slope = \left(K_m^A + K_i^A \cdot \frac{K_m^B}{b} \right) \left(\frac{1}{V_{max}} \right)$$

Equation 7

$$Intercept = \left(1 + \frac{K_m^B}{B} \right) \left(\frac{1}{V_{max}} \right)$$

Equation 8

The slope and intercept for a ping-pong mechanism at fixed concentration of 'b', using Equation 6 are described below.

$$Slope = \left(\frac{1}{V_{max}} \right) \left(\frac{1}{a} \cdot K_m^A \right)$$

Equation 9

$$Intercept = \left(\frac{1}{V_{max}} \right) \left(1 + \frac{K_m^B}{b} \right)$$

Equation 10

In the work described herein, BmaI1 was assayed using fixed concentration of one of the substrate while varying the other. The effect of change in concentration of fixed substrate on the slope and intercept of a double reciprocal plot revealed if the BmaI1 mechanism for acyl-ACP and SAM substrates is ping-pong or random/sequential. The patterns of the lines from the experimental data predicted bisubstrate kinetic mechanisms. Parallel line patterns are usually indicative of a ping-pong mechanism. Since Equation 2 for ping-pong mechanisms does not have the $K_i^A K_m^B$ term, the equation

for slope becomes independent of fixed substrate concentration, 'b'. Therefore, the slope

is unaffected upon change in 'b' and a parallel line pattern results (Equation 9).

Intersecting lines (Fig. 12) indicate a sequential/random mechanism (Equation 7 and 8).

It is important to note, however, that if the K_i^A is small compared to the K_m^A, then

parallel lines will result for a sequential and random mechanism.
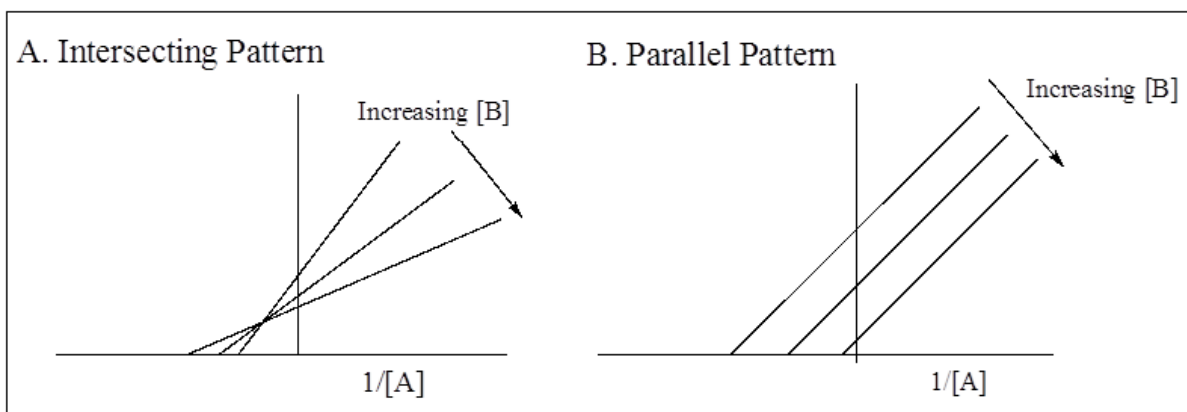
Figure 12. **Line-Weaver Burk Plots**. Enzyme assays are performed using fixed concentration of one of the substrates (B in this figure), while varying the other. Each line in this plot corresponds to a specific concentration of B. As B varied between experiments, either the slope or intercept or both will change depending on the mechanism of addition of two substrates. Parallel lines do not have slope effects, whereas intersecting lines show a slope effect. If lines intersect at a point other than the Y-axis, then an intercept effect results.

Thesis Objectives

The primary objectives in this thesis are to address the following questions:

a) Does precipitation and re-suspension affect acyl-ACP activity with BmaI1 AHL-

synthase?

b) Does BmaI1 activity change with different SAM formulations, such as SAM-chloride

and SAM-tosylate?

c) How does acyl-ACP substrate activity change with acyl chain length? How does the catalytic efficiency of a shorter or longer chain acyl-ACP substrate compare with native substrate?

d) Does the kinetic mechanism for BmaI1 change between specific and nonspecific substrates? If this is true, can we get additional insight on how this enzyme discriminates between specific and nonspecific acyl-ACP substrate?

This is the first study to report differences in rates and mechanism for nonspecific acyl-ACP substrate reacting with an AHL-synthase. The BmaI1 substrate specificity study described in this thesis is the first step towards solving the mystery of how AHL-synthase enzymes achieve tight signal specificity in bacterial QS.

CHAPTER TWO: MATERIAL AND METHODS

Materials and Equipment

All chemicals used for these projects were purchased from Sigma Aldrich. All acyl-ACPs were purchased from Life Science Resource Corp. PD10 columns were purchased from GE Life Sciences. All UV-Vis spectrophotometric data was obtained using a Thermo Scientific Evolution 260 Bio UV-Vis spectrophotometer. All samples were analyzed in Fisher 1 cm path length quartz cuvettes (14-385-928C). HPLC data was obtained using a Thermo Scientific Accela HPLC system along with a Thermo Scientific Hypersil Gold C18 reverse-phase UHPLC column (25002-054630). Transformation occurred using a BTX ECM 630 electroporator from Dr. Cornell's lab at Boise State University.

Transformation of BmaI1 Plasmid

A vial containing *E. coli* Turner DE3 competent cells (~20 µL) was placed on ice along with the BmaI1 plasmid was obtained from Professor Greenberg's laboratory at the University of Washington. Electro-cuvettes were cooled for a minimum of 10 minutes at -20 °C. Once the competent cells were thawed (in a sterile environment), the plasmid (1 µL) was added to these cells. The ligation/plasmid mixture was transferred to the cooled electro-cuvettes and inserted into the electroporator. A pulse was applied for transformation to occur (standard conditions were applied to the electroporator for transformation). Immediately after the pulse, sterile LB broth (20 µL) was added to the

cuvette and this solution was transferred to an Eppendorf tube. This was placed in a shaker for one hour at 37 °C, 225 RPM for growth. The turbid solution was partitioned and plated onto agar plates with streptomycin antibiotic selection (100 µg/mL).

BmaI1 Growth, Expression, and Purification

Two liters of Luria Bertani broth with 100 µg/mL streptomycin were inoculated with BmaI and grown at 37 °C to an OD_{600} of 0.5-0.6. Expression was then induced by addition of 0.5 mM IPTG. Growth cultures were then cooled to 16 °C and allowed to express and grow overnight. Growth cultures were then centrifuged at 4,500 x g at 4 °C for 15 minutes to pellet cells and stored at -20 °C prior to lysis. Cell pellets were thawed on ice for 45 minutes prior to lysis. The cell pellet was suspended in 2 mL of B-PER reagent was added per liter of growth to re-suspend pellet. 20 µL of (1 mg/mL) DNase and RNase and 25 µL of (13 mg/750 µL IPA) phenylmethylsulfonyl fluoride (PMSF) were added per liter of culture. Lysate was incubated at room temperature for 15 minutes under gentle shaking before centrifugation at 13,000 x g for 10 minutes. Supernatant was collected and stored on ice prior to purification. Purification was done via Ni^{2+} NTA affinity chromatography. Ni^{2+} NTA column was equilibrated using 0.5M NaCl in 50 mM Tris/HCl, pH 7.5 (Buffer A). Supernatant was loaded onto the Ni^{2+} NTA column and washed with 10 mL of 50 mM imidazole in Buffer A. BmaI1 was eluted from the column using 10 mL of 300 mM imidazole in Buffer A. Presence and purity of BmaI1 was confirmed via SDS-PAGE analysis. Concentration was determined using UV-Vis (ε_{280} = 29450 $M^{-1}cm^{-1}$).

Preparation of Precipitated ACP

Transformation of the ACP DK574 with pJT94 into BL21 *E. coli* competent cells was peformed using the same conditions as the BmaI1 transformation discussed above.

Strain DK574 with pJT94 was grown in LB broth media with 15 µg/mL kanamycin, 50 µg/mL streptomycin, 50 µg/mL spectinomycin, and 10 µg/mL chloramphenicol. Acyl carrier protein and AcpH are induced by the addition of 100 µM IPTG and incubation for another 3 to 4 hours. Cells were collected by centrifugation, which were frozen for storage at -80 °C. The cell pellets were suspended in 2 mL B-PER per liter of culture, 40 µL lysozyme per 1 liter of culture, 20 µL DNAse per liter of culture, and 60 µL PMSF per liter of culture. This was kept at room temperature for 15-20 minutes to lyse the cells. The lysate was cleared by centrifugation at ~13,000 x g for 30 minutes. $MgCl_2$ was added to 25 mM and $MnSO_4$ was added to 1.2 mM final concentration. The cleared lysate was incubated at 37 °C for 4 hours to convert all acyl-carrier protein to the apo-ACP form. Cellular protein was precipitated by the slow addition of isopropanol to 50% with mixing and was incubated on ice for 1 hour. The precipitated protein was removed by centrifugation at 10000 x g for 20 minutes. The supernatant was stirred with 6 mL of de-fined Whatman DE52 diaminoethyl cellulose per liter of culture overnight (ON). The media was packed into a column and washed with 10 column volumes of 10 mM lithium 4-morpholineethanesulfonate (MES) pH 6.1, 0.25 M LiCl and eluted with 10 column volumes of 10 mM lithium MES pH 6.1, 0.5 M LiCl. Fractions containing pure protein indicated by SDS PAGE were pooled and precipitated by addition of 0.02% sodium deoxycholate and 5% trichloroacetate and incubation for 30 minutes. The suspension was pelleted by centrifugation at 14000 x g for 30 min and apo-

ACP was resuspended in 0.5 M Tris-HCl pH 8.0. The suspended protein was then desalted using PD10 column, concentrated (ε_{280} = 1490 $M^{-1}cm^{-1}$) using a 3 kD molecular weight cutoff (MCO) spin filter column, and stored at -80 °C.[46]

Preparation of Unprecipitated ACP

Strain DK574 with pJT94 was grown in LB broth media with 15 µg/mL kanamycin, 50 µg/mL streptomycin, 50 µg/mL spectinomycin, and 10 µg/mL chloramphenicol. Acyl carrier protein and AcpH are induced by addition of 100 µM IPTG and incubation for another 3 to 4 hours. Cells were collected by centrifugation, which were frozen for storage at -80 °C. The cell pellets were suspended in 2 mL B-PER per liter of culture, 40 µL lysozyme per 1 liter growth, 20 µL DNAse per liter growth, and 60 µL PMSF per liter of culture. This was kept at RT for 15-20 minutes to lyse the cells. The lysate was cleared by centrifugation at ~13,000 x g for 30 minutes. $MgCl_2$ was added to 25 mM and MnSO4 was added to 1.2 mM final concentration. The cleared lysate was incubated at 37 °C for 4 hours to convert all acyl carrier protein to the apo-ACP form. Cellular protein was precipitated by the slow addition of isopropanol to 50% with mixing and was incubated on ice for 1 hour. The precipitated protein was removed by centrifugation at 10000 x g for 20 minutes. The supernatant was stirred with 6 mL of de-fined Whatman DE52 diaminoethyl cellulose per liter growth ON. The media was packed into a column and washed with 10 column volumes of 10 mM lithium 4-morpholineethanesulfonate (MES) pH 6.1, 0.25 M LiCl and eluted with 10 column volumes of 10 mM lithium MES pH 6.1, 0.5 M LiCl. Fractions containing pure protein indicated by SDS PAGE were pooled and desalted using PD10 column. This was then

concentrated (ε_{280} = 1490 M^{-1}cm^{-1}) using a 3 kD MCO spin filter column and stored at

stored at -80 °C.

Preparation of Unprecipitated acyl-ACP

Phosphopanetheinyl transferase, Sfp from Bacillus subtilis, was used to modify

apo-ACP with acyl-CoAs to yield acyl-ACPs. The 2 mL transferase reaction contained

50 mM Tris-HCl pH 6.8, 10 mM magnesium chloride, 750 µM apo-ACP, 937 µM acyl-

CoA (1.25X apo-ACP), and 3 µM Sfp. Acyl-CoAs were added last. For acyl-CoAs with

carbon chain lengths greater than eight, precipitation occurs and stops the reaction from

going to completion. Therefore, the volume of C10-CoA was partitioned and added to

the solution over 15 minute intervals. This reaction was incubated at 37 °C and

monitored by UHPLC for completion. The reaction time varied from 15 minutes to 2.5

hours. Then, ammonium sulfate at 75% saturation was added to the solution for 1 h at 4

°C and Sfp was precipitated and collected by centrifugation (13,000 x g for 15 minutes).

The clear acyl-ACP solution was desalted by multiple washes using a 3kD MCO spin

filter column. The desalted acyl-ACP was concentrated using a 3kD MCO spin filter

column and stored at -80°C.

Preparation of Precipitated acyl-ACP

Phosphopanetheinyl transferase, Sfp from *Bacillus subtilis*, was used to modify

apo-ACP with acyl-CoAs to yield acyl-ACPs. The 2 ml transferase reaction contained 50

mM Tris-HCl pH 6.8, 10 mM magnesium chloride, 750 µM apo-ACP, 937 µM acyl-CoA

(1.25X apo-ACP), and 3 µM Sfp. Acyl-CoAs were added last. For acyl-CoAs with

carbon chain lengths greater than eight like decanoyl-CoA (C10CoA) precipitation occurs

and stops the reaction from going to completion. Therefore, the volume of these acyl-CoAs were partitioned and added to the solution over 15 minute intervals. These reactions were incubated at 37 °C and monitored by UHPLC for completion. The reaction time varied from 15 minutes to 2.5 hours. Then, ammonium sulfate at 75% saturation was added to the solution for 1 h at 4 °C and Sfp was precipitated and collected by centrifugation (13,000 x g for 15 minutes). Acyl-ACP was precipitated with two volumes of acetone overnight at -20 °C. The precipitate was collected by centrifugation and briefly dried. Precipitated acyl-ACP was re-suspended in 15 mL of 25 mM Tris-HCl pH 7.5 and desalted by washing multiple times using a 3kD MCO spin filter column. The desalted acyl-ACP was concentrated using a 3kD MCO spin filter column and stored at -80 °C.

Acyl-ACP Separation Using UHPLC

Using a UHPLC analytical C18 column, acyl-ACP purification was determined. Solvent A consisted of H_2O + 0.1% TFA and solvent B consisted of acetonitrile (ACN) + 0.1% TFA. At flow rate of 600 µL/min, a gradient of 75% A and 25% B was initiated and over a ten minute period changed to 25% A and 75% B.

Electrospray Ionization Mass Spectrometry

Molecular mass of ACP and its derivatives were determined using a Bruker maxis Quadrupole-Time-of-Flight (Q-TOF) mass spectrometer equipped with an Electrospray Ionization (ESI). Ten microliter of samples were injected onto a Phenomenex C18 column (100 x 2.1 mm, 2.6µ) followed by a simple linear gradient for sample desalting and separation. The initial eluent was 98% mobile phase A (99.9% water, 0.1% formic

acid) and 2% B (99.9% acetonitrile, 0.1% formic acid) for 5 min and then mobile phase B was increased to 50% in 25 min. LC eluent was diverted to the waste during the first five minutes of the gradient to eliminate salts in the sample buffer. Mass analysis was performed using positive ion mode with a spray voltage of 4000V. Obtained mass spectra were deconvoluted using Bruker Data Analysis 4.0 software tool to obtain charge state (N) of protein ions. To calculate the molecular mass of ACP and its derivatives, the measured m/z values were multiplied by corresponding N and were subtracted by the mass of N protons (N x 1.0079). **ACP**: calculated average mass - 8508.3 Da, observed mass - 8507.5 Da; **C4ACP**: calculated mass – 8916.8 Da, observed mass – 8918.2 Da; **C6ACP**: calculated mass – 8944.9 Da, observed mass – 8946.2 Da; **C8ACP**: calculated mass – 8973.0 Da, observed mass – 8974.4 Da; **C10ACP**: calculated mass – 9000.8 Da, observed mass – 9002.3.

HPLC Method Addressing Ping-Pong Mechanistic Possibility

The experiments were conducted with using two methods. Method 1 separates apo-ACP from acyl-ACPs and indicates the RT for BmaI1. Method 1 monitors the appearance of holo-ACP and is ten minutes. Method 2 separates SAM from MTA and is a sixty minute method that monitored the appearance of MTA. Solvent A is NanoPure water + 0.1% TFA and solvent D is ACN + 0.1% TFA.

Method 1 used a 600 µL/min flow rate and started with 75% A and 25% B. Over a ten minute period the gradient changed to 25% A and 75% B. For the C8ACP/BmaI1 test, a 1:1 mixture of C8ACP and BmaI1 enzyme were mixed at 40 µM in 100 mM HEPES buffer pH 7.2. This mixture was then allowed to incubate at 37°C for 30 minutes and then an additional 30 minutes with two HPLC injects occurring at T30 and T60.

After 60 minutes, 10 µL of 12 mM SAM-Cl (sigma) was added to the reaction mixture and allowed to incubate for 10 minutes before being injected onto the HPLC.

Method 2 used a 500 µL/min flow rate and started with 100% A and 0% D. Over a ten minute period the gradient changed to 70% A and 30% D. For the SAM-Cl (Sigma)/BmaI1 test, a mixture of SAM-Cl (Sigma) and BmaI1 were mixed at concentrations of 100 µM and 45 µM respectively. A control was also made with only 100 µM SAM-Cl. The reaction and control were monitored for one hour. After no change between the BmaI1 containing mixture and the control, 60 µM of C8ACP was then added to the reaction mixture and a reaction was seen.

DCPIP Assay for BmaI1

The enzymatic reaction catalyzed by BmaI was monitored using a colorimetric assay that is sensitive to the free thiol generated upon transfer of the acyl group from either C8ACP or various acyl-ACPs. A typical reaction contained 30 uM DCPIP and 100 mM HEPES, pH 7.2. For C8ACP determination of K_m and k_{cat}, SAM was fixed at 3 mM while C8ACP varied from 2-100 µM. For determination of K_m and k_{cat} for SAM, C8-ACP was fixed at 25-30 µM. For generating curves with different acyl-ACP varying, SAM was fixed at 3 or 6 mM while the acyl-ACP concentrations varied from 2-100 µM. For generating curves with SAM varying, acyl-ACP was kept at 5-10X the acyl-ACP's K_m. SAM, acyl-ACP, buffer, and DCPIP was incubated for 25 minutes before initiating with enzyme to eliminate background rates. Reactions were initiated by the addition of BmaI1 (200 nM for C8ACP, 560 nM C6ACP, 960 µM C10ACP and 2.86 µM C4ACP, and 5 µM C8CoA). The thiol-dependent reduction of DCPIP was monitored at 600 nm

$(\varepsilon = 21000 \text{ M}^{-1}\text{cm}^{-1})$ for no more than 800 seconds. The initial rate data was fit to

Michaelis-Menten (Equation 3) or substrate inhibition equation using GraphPad Prism

6.0. All experiments were done in triplicate to check for reproducibility and to estimate

errors.

CHAPTER THREE: RESULTS AND DISCUSSION

Enzyme Purification

<u>BmaI1</u>

The appearance of small white circular colonies on the streptomycin antibiotic selected

(100 µg/mL) agar plates confirmed that the transformation of BmaI1 into *E. coli* Turner

DE3 cells using electroporation was successful. Colonies were used to inoculate large

volumes of medium with streptomycin antibiotic selection (100 µg/mL). The large

culture reached $OD_{600} = 0.5$-0.8 within three hours of inoculating. Chemical lysing using

B-PER, DNase, RNase, and PMSF was fast and efficient in producing clear yellow lysate

(compared to sonication). The BmaI1 plasmid that was provided by Dr. Peter

Greenberg's lab contained a 6-His tag for Ni-NTA affinity chromatography purification.

The molecular weight (MW) of BmaI1 using this sequence is 22938.1Da (Fig. 13A). It is

expected that fractions containing BmaI1 would show banding at ~23 kD. Analysis of

SDS-PAGE confirmed BmaI1 was isolated from Ni-NTA chromatography at ~23 kD

(Fig. 14).

A

```
        10        20        30        40        50        60
  MRTFVHGDGR LPSDLAADLG LYRHGVFVEQ LGWKLPSASE GFERDQYDRD DTVYVFARDD


        70        80        90       100       110       120
  DGEICGCARL LPTTRPYLLK ELFPTLVAQD MPLPQSAAVW ELSRFAANAE DPAGGGNPAW


       130       140       150       160       170       180
  AVRPMLAAVV ECAARLGAKQ LIGVTFLSME RLFRRIGVHA HRAGPAQQID GRMVVACWID


       190       200
  LDAQTLAALD LDPLLCAPPA EAA
```

B

```
        10        20        30        40        50        60
  MSTIEERVKK IIGEQLGVKQ EEVTNNASFV EDLGADSLDT VELVMALEEE FDTEIPDEEA


        70
  EKITTVQAAI DYINGHQA
```

Figure 13.   Amino Acid Sequences for BmaI1 (A) and apo-ACP (B).   Using Protparam the MW for BmaI1 and apo-ACP was calculated to be 22115.2 Da and 8639.5 Da, respectively. Adjusting for the 6-His tag added to this sequence the MW is predicted to be 22938.1 Da.
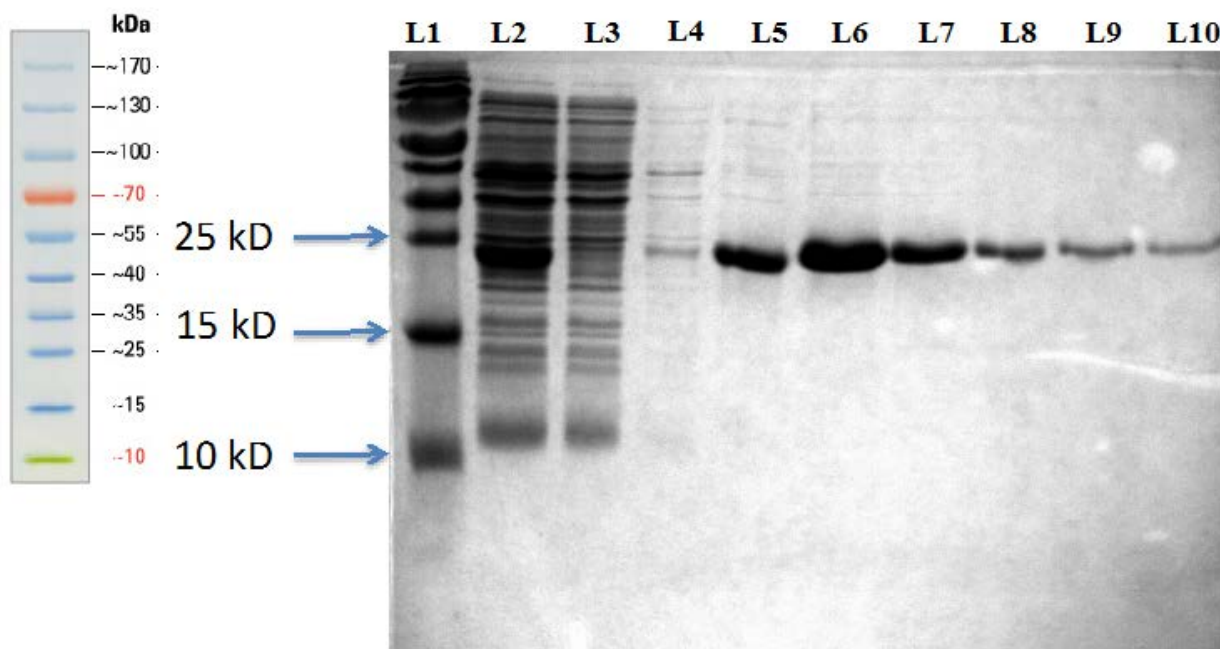
Figure 14. **SDS-PAGE of BmaI1 2L culture using Ni-NTA chromatography:** Lane 1 (L1): EZ prestained protein ladder; Lane 2 (L2): Crude BmaI1; Lane 3 (L3): BmaI1 Load; Lane 4 (L4): 50 mM imidazole in Tris-HCl buffer wash of BmaI1; Lane 5-10 (L5-L10): 200 mM imidazole in Tris-HCl buffer Elutions 1-6. BmaI1: MW - 22938.1 Da. The 25 kD marker is the third line up from the bottom and the elutions in lanes 5-10 are slightly below the 25 kD marker. These bands are around 23 kD and were concentrated to 1.5 mL at 97 µM.

<u>Apo-ACP (Precipitated and Unprecipitated)</u>

The appearance of small white circular colonies on agar plates with the

kanamycin (15 µg/mL), streptomycin (50 µg/mL), spectinomycin (50 µg/mL), and

chloramphenicol (10 µg/mL) antibiotic selection confirmed the transformation of apo-

ACP into BL21 *E. coli* competent cells using electroporation was successful. Colonies

were used to inoculate large growths with the same antibiotic selection as the plates. The

culture reached $OD_{600} = 0.5\text{-}0.8$ within four hours of inoculating. Chemical lysing using

B-PER, DNase, RNase, lysozyme, and PMSF was fast and efficient in producing clear

yellow lysate (compared to sonication). All cells produce holo-ACP during fatty acid

biosynthesis and thus when isolating apo-ACP there is always holo-ACP contamination.

Since these two proteins are similar in structure and molecular weight, separating one

from the other is a laborious process. Therefore, Dr. Peter Greenberg's lab included an

additional gene, ACPH (ACP-hydrolase), in the plasmid that converted holo-ACP to apo-

ACP by the addition of $MgCl_2$ and $MnSO_4$ to the clear lysate. The conversion of holo-

ACP to apo-ACP produces a cloudy lysate. ACP hydrolase was precipitated with IPA

and gave a white solid. Removal of ACP hydrolase with centrifugation yielded a clear

lysate. Anion exchange chromatography was used to successfully isolate pure fractions

of apo-ACP from other cellular debris. The amino acid sequence of apo-ACP is shown

in Fig. 13B and this sequence has a MW of 8639.5 Da. It is expected that fractions

containing apo-ACP would show banding at ~9 kD. Analysis of SDS-PAGE confirmed

that apo-ACP was isolated by anion exchange chromatography at ~9 kD (Fig. 15).
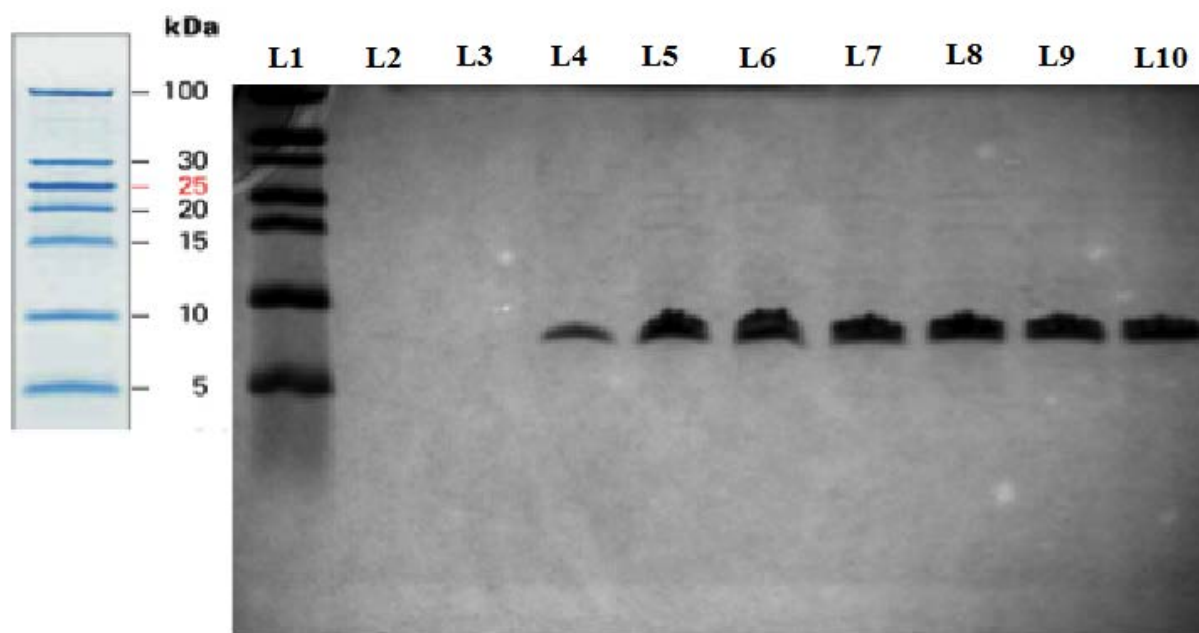
Figure 15. **SDS-PAGE of apo-ACP 2L culture using anion exchange chromatography:** Lane 1 (L1): EZ prestained low range protein ladder; Lane 2 (L2): Column wash with 10 mM MES + 0.5 mM LiCl pH 6.13; Lanes 3-10 (L3-L10) contains elutions 1-8 using10 mM MES + 0.5M LiCl pH 6.13. Apo-ACP: MW - 8639.5 Da. Apo-ACP is isolated in lanes 4-10 and were concentrated to 1.5 mL at 12 mM.

Substrate Synthesis

<u>Acyl-ACP Purification</u>

The syntheses of all acyl-ACPs were confirmed by HPLC (Fig. 16). Apo-ACP

elutes at 6.0 minutes using the Method 1 described previously. The addition of the acyl-

pantetheine linker (Fig. 17) and acyl chain to apo-ACP shifts the retention time (RT) for

each substrate accordingly.
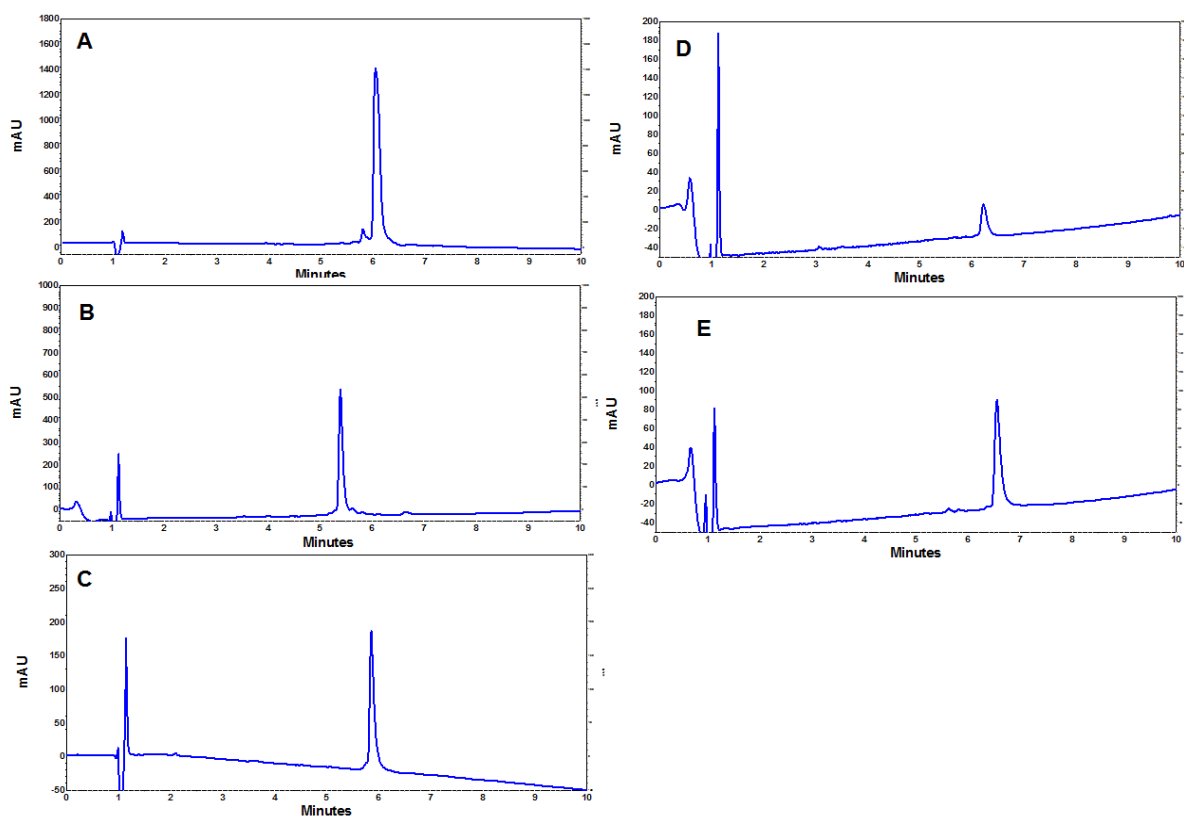
Figure 16. **HPLC chromatograms of apo-ACP and acyl-ACPs using Method 1.**
(A) Apo-ACP eluted at 6.0 minutes; disappearance of this peak was monitored over time
to confirm successful synthesis of acyl-ACPs. Contamination of holo-ACP was
monitored by the appearance of a peak at 5.2 minutes. All samples shown are free of
holo-ACP. (B) Butyryl-ACP (C4ACP) eluted at 5.5 minutes and was completed within
15 minutes. (C) Hexanoyl-ACP (C6ACP) eluted at 5.8 minutes and was completed
within 15 minutes. (D) Octanoyl-ACP (C8ACP) eluted at 6.2 minutes and was
completed within 30 minutes. (E) Decanoyl-ACP (C10ACP) eluted at 6.6 minutes and

had C10CoA partitioned over a two-hour period. After addition of all C10CoA, the reaction was complete within 30 minutes.

Enzymatic synthesis of acyl-ACPs requires the acyl-CoA stock to be pure. If the stock has free acid CoA, then holo-ACP will contaminate the reaction (Fig. 17). Holo-ACP is a product of AHL-synthase BmaI1 enzymatic reactions and can inhibit experimental rates.
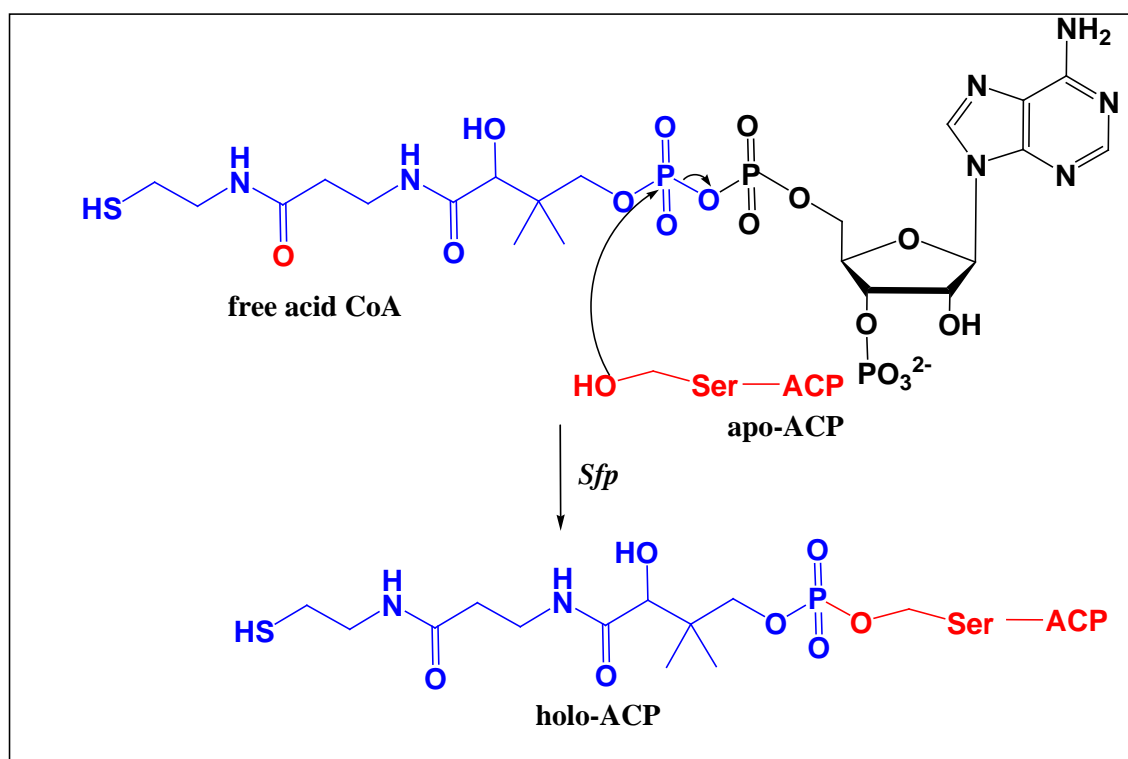
Figure 17. **Enzymatic synthesis of holo-ACP from free acid CoA, apo-ACP, and Sfp.** Free acid CoA reacts freely with apo-ACP and is converted to holo-ACP with Sfp. Holo-ACP is a product of AHL-synthase BmaI1 enzymatic reactions and can inhibit experimental rates. The portion outlined in blue is the pantetheine linker that differentiates holo-ACP from apo-ACP.

To successfully study this enzyme with acyl-ACP substrates, there cannot be holo-ACP present. Using the Method 1, holo-ACP elutes at 5.2 minutes. Each acyl-ACP used is free of holo-ACP and has distinct RTs from apo-ACP. These reactions are monitored by the depletion of the apo-ACP peak and the growth of the corresponding

acyl-ACP peak. The enzyme used for this reaction is *Sfp* and it elutes at 3.1 minutes. It is important to keep track of the final volume of the completed reaction because this volume is needed to assess the amount of ammonium sulfate needed to precipitate out *Sfp*. Once the enzyme has been removed from the reaction, multiple washes to remove excess acyl-CoA and ammonium sulfate are needed to synthesize a clean acyl-ACP substrate. These molecules absorb UV-Vis light at 260 nm whereas apo-ACP absorbs this light at 280 nm. Therefore, monitoring the reduction of the 260 nm peak during each wash determined when each acyl-ACP was free of contamination.

Acyl-ACP Characterization

The syntheses of all acyl-ACPs were successfully confirmed by MS (Fig. 18). The obtained mass spectra were deconvoluted using the Bruker Data Analysis 4.0 software tool to obtain the charge state (N) of protein ions. To calculate the molecular mass of ACP and its derivatives, the measured m/z values were multiplied by corresponding N and were subtracted by the mass of N protons (N x 1.0079). ACP can exist in two forms where a methionine residue is oxidized and where it has been truncated. Both of these forms were observed using this method. The calculated average mass of ACP is 8508.3 Da and its observed mass using this method was 8507.5 Da; C4ACP has a calculated mass of 8916.8 D and was observed at 8918.2 Da; C6ACP has a calculated mass of 8944.9 Da and its mass was observed at 8946.2 Da; C8ACP has a calculated mass of 8973.0 Da and its mass was observed at 8974.4 Da; C10ACP has a calculated mass of 9000.8 Da and was observed mass at 9002.3 Da.
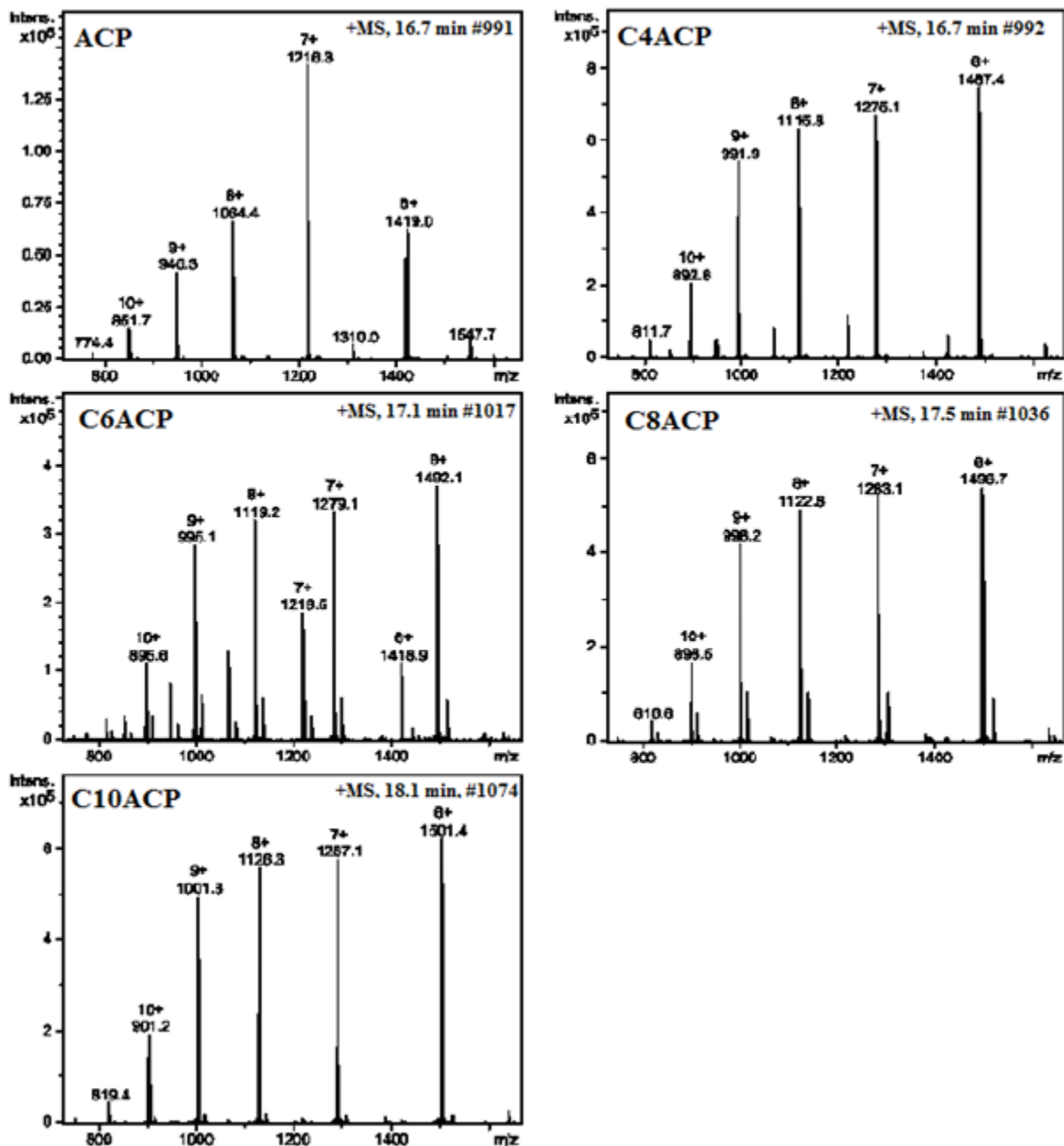
Figure 18.   ESI Mass Spectra of ACP and its derivatives in positive ion modes. ACP: calculated average mass - 8508.3 Da, observed mass - 8507.5 Da; C4ACP: calculated mass – 8916.8 Da, observed mass – 8918.2 Da; C6ACP: calculated mass – 8944.9 Da, observed mass – 8946.2 Da; C8ACP: calculated mass – 8973.0 Da, observed mass – 8974.4 Da; C10ACP: calculated mass – 9000.8 Da, observed mass – 9002.3 Da.

Effect of ACP Precipitation on Substrate Activity

Prior studies have shown that ACP conformation changes while interacting with different enzyme partners, but it has not been studied whether apo-ACP precipitation and resuspension results in subtle conformational changes in structure. We have found that the most active substrate with BmaI1 has had ACP precipitated with sodium deoxycholate and trichloroacetic acid and acyl-ACP not precipitated with the addition of acetone (Fig. 19).
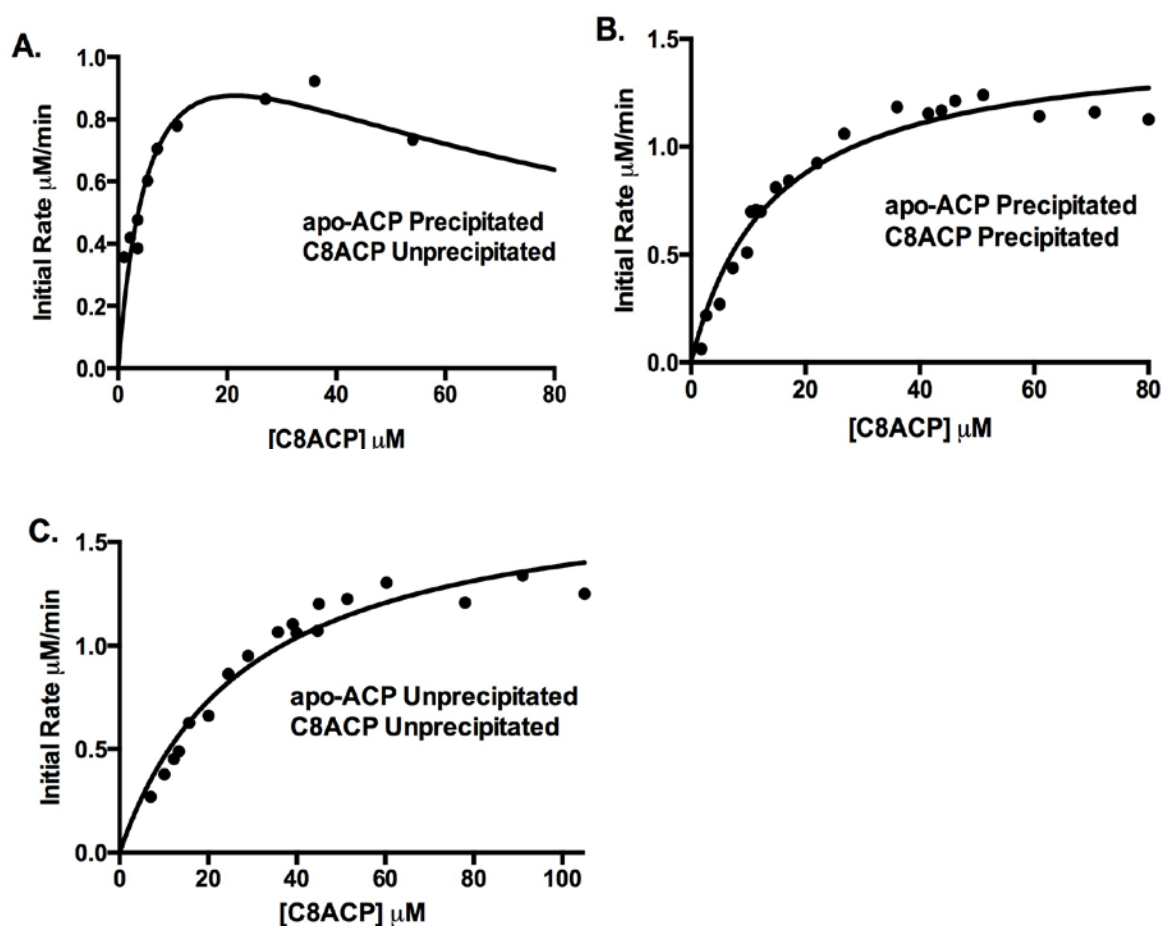
Figure 19. **Effects of ACP precipitation on BmaI1 activity.** (A) Velocity vs. [C8-ACP]; ACP was precipitated with TCA and sodium deoxycholate and C8-ACP wasn't precipitated with acetone. This preparation of substrate is the most active. (B) Velocity vs. [C8-ACP]; ACP is precipitated with TCA and sodium deoxycholate and C8-ACP was precipitated with acetone. This is the second most active preparation of substrate. (C)

Velocity vs. [C8-ACP]; ACP wasn't precipitated and the C8-ACP wasn't precipitated. This was the least active preparation of substrate.

Table 2 shows the relative % of k_{cat}/K_m for each substrate. The k_{cat} is a Michaelis-Menten parameter that can be calculated as $V_{max}/[E]$ and its units are 1/seconds. It is referred to as the 'turn-over' number and it is equivalent to the amount of substrate converted to product in one second. k_{cat}/K_m is the specificity constant referred to as the catalytic efficiency. This term explains how fast the enzyme reacts with the substrate once it encounters the substrate. Usually, the upper limit of k_{cat}/K_m is determined by the rate of diffusion because the substrate has to diffuse and collide with the enzyme and fit into the active site before it can be converted to product. For BmaI1 DCPIP assays, the catalytic efficiency is greatest for ACP precipitated and C8ACP unprecipitated. Precipitating both samples causes a 3-fold decrease in efficiency and omitting the precipitation step for proteins causes a 6-fold decrease in the efficiency.

Table 2. C8ACP preparation and determination of K_m, k_{cat}, k_{cat}/K_m, curve type, and substrate inhibition

Variable S	Fixed S	k_{cat} (min^{-1})	K_m (μM)	k_{cat}/K_m (μM^{-1})(min^{-1})	k_{cat}/K_m [#]Relative %	Curve	Substrate Inhibition
ACPP, C8ACPU	SAM-Cl	5.8 ± 0.6	6 ± 1	0.96 ± 0.18	100 %	Hyperbolic	Yes
ACPP, C8ACPP	SAM-Cl	3.7 ± 0.2	11 ± 3	0.34 ± 0.09	35 % (3-fold)	Hyperbolic	No
ACPU, C8ACPU	SAM-Cl	4.6 ± 0.5	30 ± 6	0.15 ± 0.03	16 % (6-fold)	Hyperbolic	No

k_{cat}/K_m **Relative % = [{k_{cat}/K_m}$^{acyl-ACP}$/{k_{cat}/K_m}^{ACPP,C8ACPU}]**

Effect of SAM Formulation on Substrate Activity

The commerically available formulations of SAM-Cl and SAM-tosylate were assayed with BmaI1 and C8ACP. Commercially available formulations of SAM are

known to break down into MTA and HSL, which have the potential to inhibit BmaI1

activity. Additionally, the anionic salts that stabalize SAM such as chloride and tosylate

can affect the activity of BmaI1. Tosylate is a bulky conjugated compound compared to

chloride (Fig. 20). The anionic salts could bind to BmaI1 and produce conformational

changes that could inhibit the enzyme's ability to turn over C8ACP.
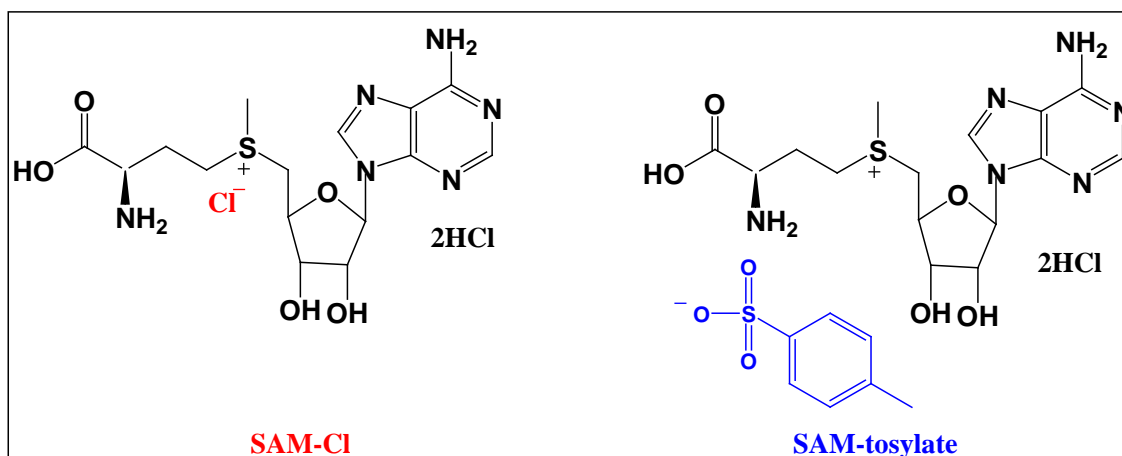
Figure 20.   SAM-chloride and SAM-tosylate structures.   All commercially
available formulations of SAM are stored in acidic conditions. SAM-Cl has a small
anionic chloride while SAM-tosylate contains a larger MW salt that is conjugated.

When testing SAM-Cl and SAM-tosylate, K_m and k_{cat} values were not

differentiable in comparison (Fig. 21). SAM-Cl K_m is 1.8 ± 0.3 mM and SAM-tosylate is

0.9 ± 0.2 mM. The k_{cat} for SAM-Cl is 5.8 ± 0.8 min^{-1} and for SAM-tosylate it is 6.2 ± 0.4

min^{-1}. BmaI1 activity doesn't change with different SAM formulations such as SAM-

chloride and SAM-tosylate. This indicates that either substrates can be used with the

DCPIP assay to study BmaI1. This is advantageous for laboratories that are restricted to

purchasing formulations of SAM when studying AHL-synthases. Interestingly, SAM-

tosylate at concentrations greater than 3 mM indicated decreased rates. The IC$_{50}$ of

tosylate was tested and indicated inhibition occurring at 1 mM.
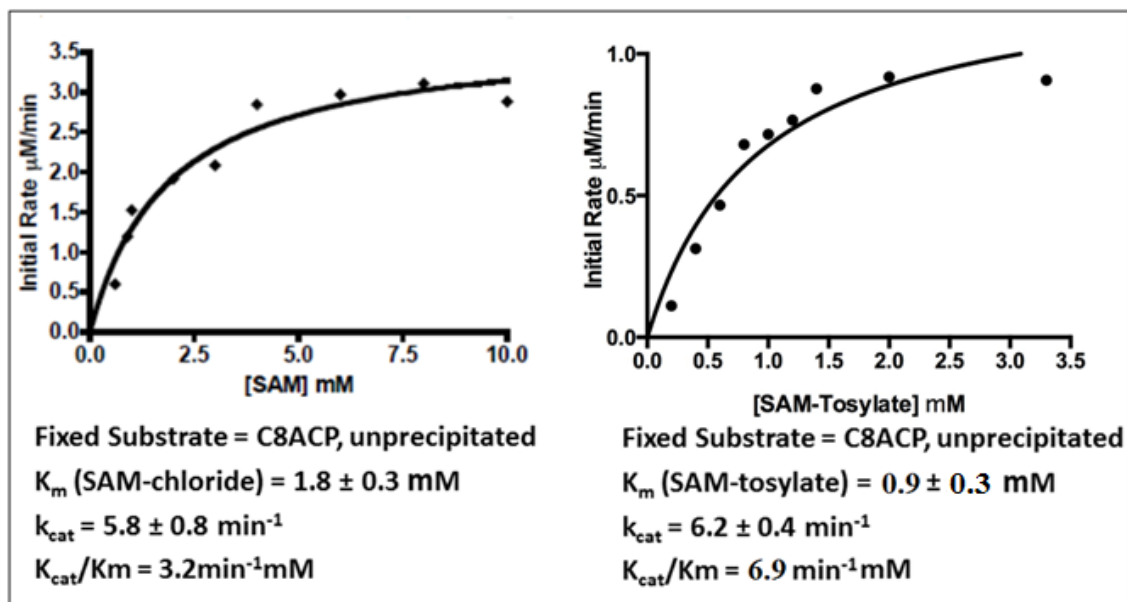
Figure 21. **Effects of SAM formulations on BmaI1 activity.** Both assays were initiated with 200 nM BmaI1. A. SAM-Cl was used as the variable substrate and C8ACP unprecipitated was fixed at 20 µM. Km (SAM-chloride) is 1.8 ± 0.3 mM; kcat is 5.8 ± 0.8 min-1; kcat/Km is 3.2min-1mM. B. SAM-tosylate was used as the variable substrate and C8ACP unprecipitated was fixed at 20 µM. Km (SAM-tosylate) is 0.9 ± 0.2 mM; kcat is 6.2 ± 0.4 min-1; kcat /Km is 6.9 min-1mM. SAM-tosylate at concentrations greater than 3 mM indicated decreased rates. The IC_{50} of tosylate was tested and indicated inhibition occurring at 1 mM.

Exploring the Kinetic Mechanism of BmaI1

<u>DCPIP assay of BmaI1, C8ACP, and SAM</u>

Plotting the double reciprocal of variable concentration of C8ACP and fixed concentrations of SAM-Cl displayed a series of parallel lines (Fig. 22). Parallel line patterns are indicative of a ping-pong mechanism (Fig. 23).
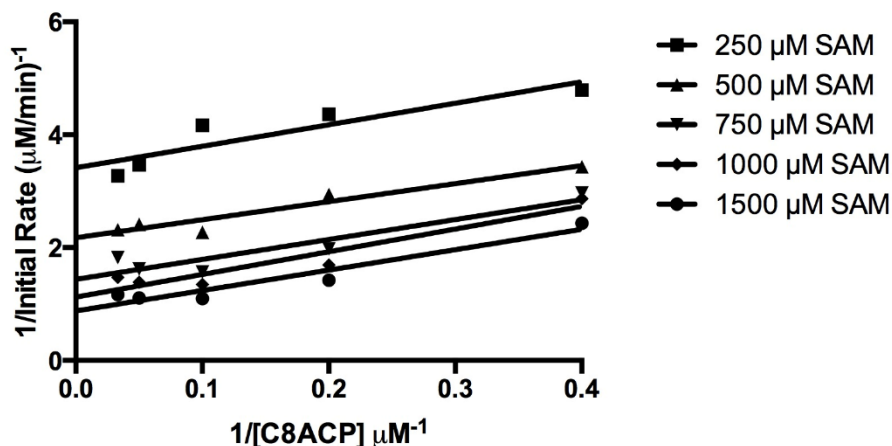
Figure 22. **Double Reciprocal Plot of BmaI1, C8ACP, and SAM using the DCPIP Assay.** These assays are accomplished using variable concentrations of C8ACP ranging from 0-100 µM while fixing SAM. Five assays were completed using different concentrations of SAM-Cl ranging from 250-1500 µM. The K_i^A of C8ACP is 125 ± 43 nM. Plotting the double reciprocal of the data generates a series of parallel lines. This indicates the enzymatic mechanism is ping-pong.[47]
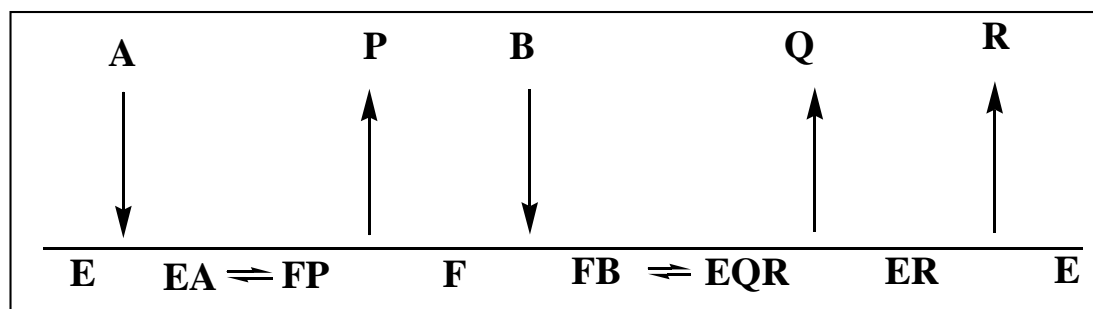
Figure 23. **Ping-Pong Mechanism for bi-substrate Kinetics**

The double reciprocal Michaelis-Menten equation for a bisubstrate ping-pong

mechanism is

$$\frac{1}{V_0} = \frac{1}{V_{max}}\left[\left(1 + \frac{K_m^B}{b}\right) + \frac{1}{a}\left(K_m^A\right)\right] \qquad \text{Equation 1}$$

The slope and intercept for a ping-pong mechanism is

$$Slope = \left(\frac{1}{V_{max}}\right)\left(\frac{1}{a}.K_m^A\right) \qquad \text{Equation 2}$$

$$Intercept = \left(\frac{1}{V_{max}}\right)\left(1 + \frac{K_m^B}{b}\right) \qquad \text{Equation 3}$$

Ping-pong mechanisms slope becomes independent of fixed substrate concentration. In this case, SAM-Cl was fixed while varying C8ACP. At times, parallel lines can result for sequential and random mechanisms. The double reciprocal Michaelis-Menten equation for these mechanisms is

$$\frac{1}{V_0} = \frac{1}{V_{max}} \left[\left(1 + \frac{K_m^B}{b} \right) + \frac{1}{a} \left(K_m^A + K_i^A \cdot \frac{K_m^B}{b} \right) \right] \qquad \text{Equation 4}$$

Parallel lines for random and ordered sequential mechanisms occur when the K_i^A is small compared to the K_m^A. This study obtained the K_i^A for C8ACP to be 125 ± 43 nM and the K_m^A for C8ACP is 6 ± 1 μM. The K_i^A is much less than the K_m^A, which suggests that further experimentation is needed before deciding the mechanism is ping-pong.

Eliminating Ping-Pong Mechanism

A bi-substrate ping-pong mechanism involves one substrate adding to the enzyme and converting to product immediately (Fig. 23). Therefore, if BmaI1 follows this mechanism, when incubating BmaI1 with C8ACP product release should be observed. Since acylation is dependent on the acyl-ACP substrate, holo-ACP is the expected product to be released when incubating with only C8ACP (Fig. 24A). Lactonization is dependent on the substrate, SAM, and HSL and MTA are the expected products to be released when incubating only with SAM-Cl (Fig. 24B).
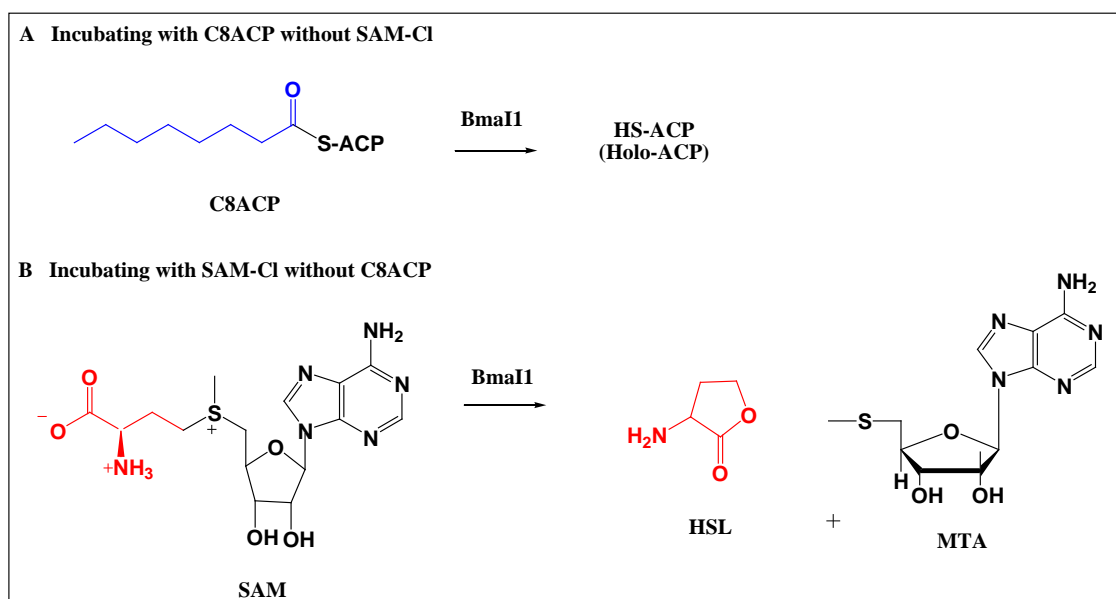
Figure 24. **Expected Products when C8ACP is incubated with BmaI1 without SAM-Cl (A) and when SAM-Cl is incubated with BmaI1 without C8ACP (B).** Holo-ACP can only be released when C8ACP is acylated in the active site of BmaI1. When incubating with only SAM-Cl lactonization alone can produce HSL and MTA.

Incubating SAM, C8ACP, and BmaI1 and injecting a sample for HPLC analysis showed C8ACP depletion and holo-ACP turned over (Fig. 25A). Studying SAM-Cl turnover is more difficult because the commercially available SAM-Cl can break down into MTA. This means that there is a starting amount of MTA existing before enzyme is added. In order to observe the amount of MTA that has naturally broken down from SAM-Cl, the enzyme Methylthioadenosine/S-adenosylhomocysteine (MTA/SAH) nucleosidase (MTN) was added. MTN catalyzes the irreversible cleavage of the glycosidic bond in both 5'-methylthioadenosine (MTA) and S-adenosylhomocysteine (SAH) to adenine and the corresponding thioribose, 5'-methylthioribose and S-ribosylhomocysteine, respectively. When injecting 100 µM SAM-Cl with 1.6 µM MTN over 45 minutes, there was no significant peak area change observed. Therefore SAM and adenine seem to be stable under the reaction conditions (Fig. 26A and Table 3 and 4). When BmaI1 was added to this sample, there was no significant change in peak area for

SAM or adenine (Fig.26B). Adding C8ACP to this reaction showed a decrease in adenine

peak (Fig. 26C). Table 3 and 4 is a compilation of the quantitative data and sample

definitions for these experiments (Fig. 26). When incubating C8ACP and SAM

independently with BmaI1, there was also was no change in the chromatogram,

indicating the expected product of the ping-pong mechanism wasn't produced (Fig. 25B).

Therefore, the mechanism must be random or ordered sequential.
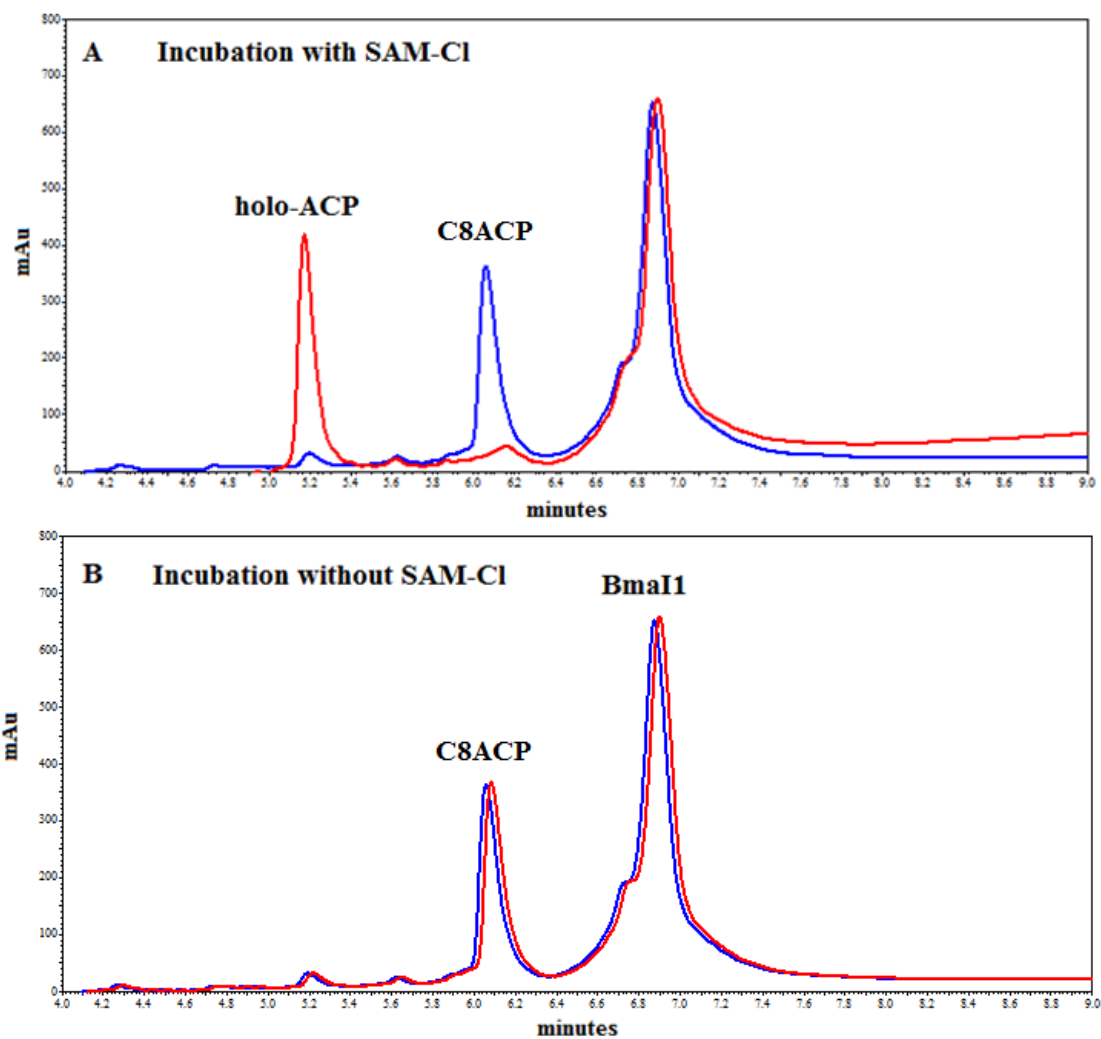
Figure 25. **HPLC chromatogram using Method 1:** (A) Chromatogram showing 40 µM C8ACP and 40 µM BmaI1 incubated at time 30 (Blue) and the same reaction + 1.2 mM SAM at time 90 (red). Near complete conversion of the C8ACP to holo-ACP is seen indicating active enzyme. C8ACP elutes at 6.15 minutes, holo-ACP at 5.2 minutes, and BmaI1 at 6.75 minutes. (B) Chromatogram showing 40 µM C8ACP and 40 µM BmaI1 incubated at time 30 (Blue) and time 60 (red). There is no decrease in the C8ACP peak nor any holo-ACP. Method 1 used a 600 µL/min flow rate and started with 75% A and 25% B. Solvent A is NanoPure water + 0.1% TFA and solvent D is ACN + 0.1% TFA.[47]
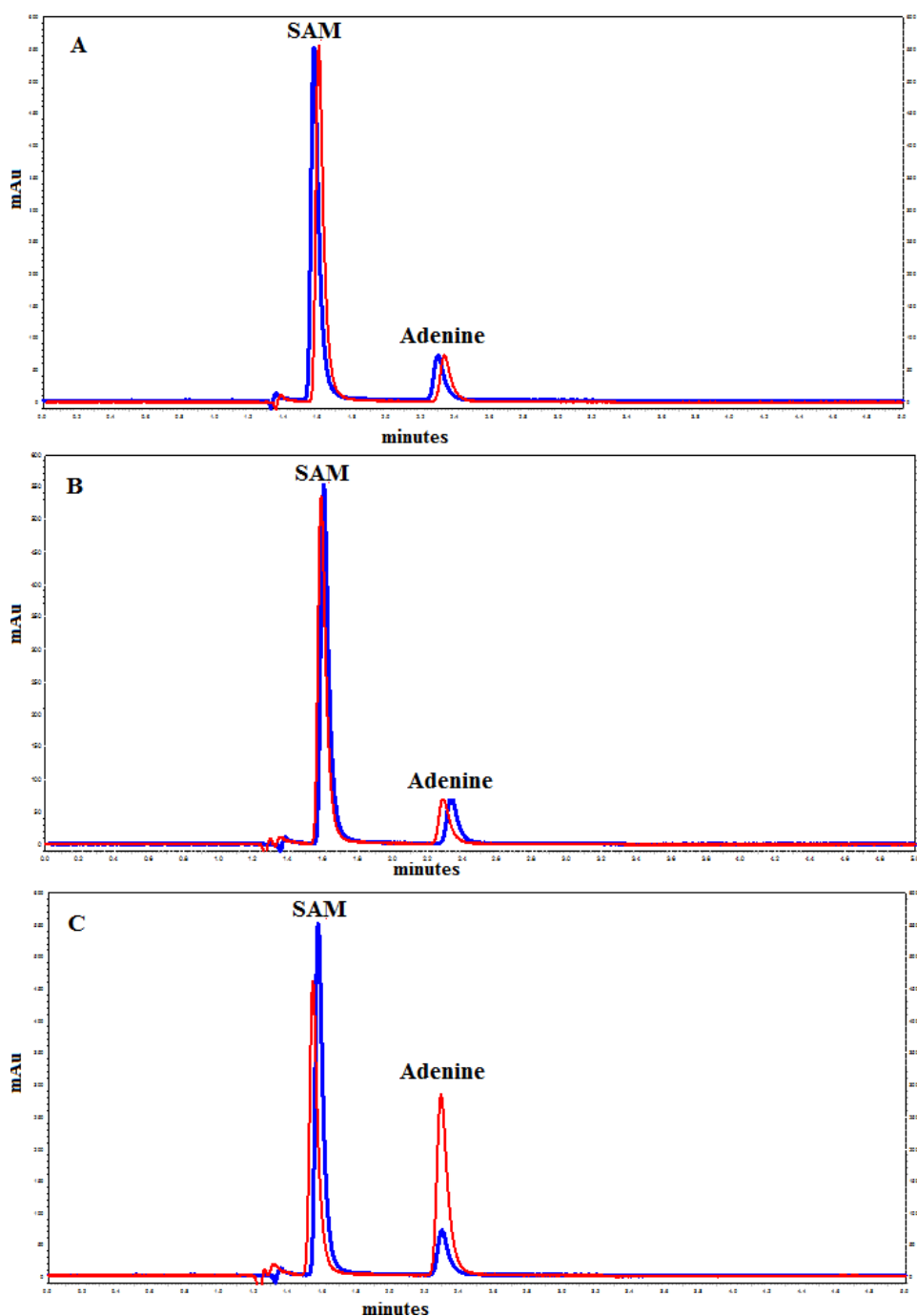
Figure 26. **HPLC Chromatograms using Method 2:** (A) Chromatogram of Control showing 100 µM SAM-Cl and 1.6 µM MTN at time 0 (blue) and time 45 (red). No significant peak area change is seen. Therefore, SAM and adenine seem to be stable in reaction. (B) Chromatogram of Control at time 45 (Blue) and 19. 4 µM of BmaI1 reaction at T60 (Red). No significant change in peak area for SAM or adenine is seen. (C) Chromatogram of control reaction at time 60 (Blue) and BmaI1 reaction + 60uM C8ACP at time 80 (Red). A significant decrease in SAM area is seen along with a significant increase in the adenine peak as expected. Method 2 used a 500 µL/min flow rate and

started with 100% A and 0% D Solvent A is NanoPure water + 0.1% TFA and solvent D is ACN + 0.1% TFA.[47]

Table 3.   Ping-pong mechanism experiment quantitative analysis with arbitrary peak areas[47]

	Run					
Compound	100 µM SAM	100 µM SAM+ 1.6 µM MTN	Control T0	Control T45	BmaI1 Rxn T60	BmaI1 Rxn + 60 µM C8ACP
SAM-Cl	18.0271	18.7008	18.4890	18.8234	18.4155	11.7485
MTA	2.8326	0	0	0	0	0
Adenine	0	3.23526	3.16584	3.3975	3.16434	9.4819
SAH	0.3673	0	0	0	0	0
SAM/Adenine	NA	5.7803	5.8401	5.5403	5.81970	1.2390

Table 4.   Ping-pong mechanism experiment sample definitions[47]

	Control	**BmaI1 Reaction**	**BmaI1 Rxn + C8-ACP**
SAM:	100 µM	100 µM	100 µM
MTN:	1.6 µM	1.6 µM	1.6 µM
BmaI1:	0 µM	19.4 µM	19.4 µM
HEPES Buffer:	100 mM	100 mM	100 mM
C8-ACP	0 µM	0 µM	60 µM

Acyl-Chain Length Specificity

To determine if BmaI1 activity changes with acyl chain length, four substrates (C4ACP, C6ACP, C10ACP, and C8CoA) with variable concentrations were assayed with SAM-Cl fixed. Figure 27 is a compilation of the Velocity vs. [Substrate] curves generated using this approach. The appropriate enzyme concentration was determined first by varying BmaI1 with saturating concentrations of both substrates. Incubating DCPIP, SAM, acyl-ACPs, and C8CoA for 25 minutes depleted background rates. The K_m and k_{cat} terms were used to determine activity.
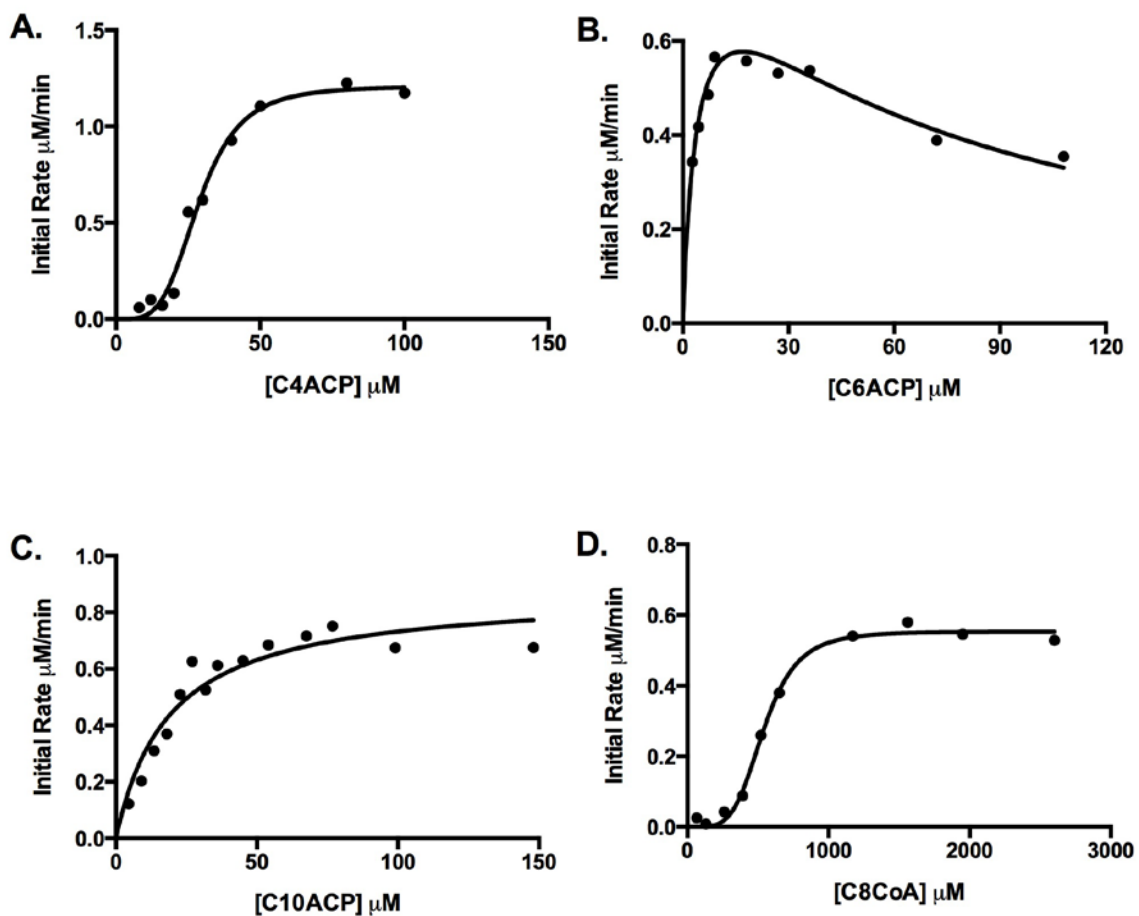
Figure 27. **Substrate-velocity curves for nonspecific acyl-ACP substrates reacting with BmaI1.** Initial rate as a function of substrate concentration for 3 mM SAM chloride (fixed) and (A) varying C4ACP in 2 μM BmaI1 (B) varying C6ACP in 0.56 μM BmaI1 (C) varying C10ACP in 1 μM BmaI1 and (D) varying C8CoA in 5 μM BmaI1. The rate curves were sigmoidal for poor substrates (C4ACP, C8CoA) and hyperbolic for C6ACP and C10ACP substrates. The dissociation constant for C6ACP substrate inhibition is 69 ± 14 μM. Deviation from Michaelis-Menten behavior for C4ACP and C8CoA are indicative of kinetic cooperativity. Positive cooperativity (Hill slope > 1) was observed for both of these substrates. Acyl-ACP substrates were enzymatically synthesized from apo-ACP and acyl-CoA. While apo-ACP was precipitated, all acyl-ACP samples (C4ACP, C6ACP, and C10ACP) were prepared by omitting the acetone precipitation step in substrate purification. C6ACP and C10ACP substrate-velocity data was fit to substrate inhibition equation and Michaelis-Menten equation, respectively, while C4ACP and C8CoA rate data was fit to Hill equation.

To understand if structural changes in fixed acyl-ACP substrates affected SAM activity, four nonspecific acyl-ACP substrates (C4ACP, C6ACP, C10ACP, and C8CoA) were fixed and assayed with variable concentrations of SAM-Cl.   Figure 28 is a

compilation of Velocity vs. [Substrate] curves generated using this approach. The appropriate enzyme concentration was determined first by varying BmaI1 with saturating concentrations of both substrates. Incubating DCPIP, SAM, acyl-ACPs, and C8CoA for 25 minutes depleted background rates.
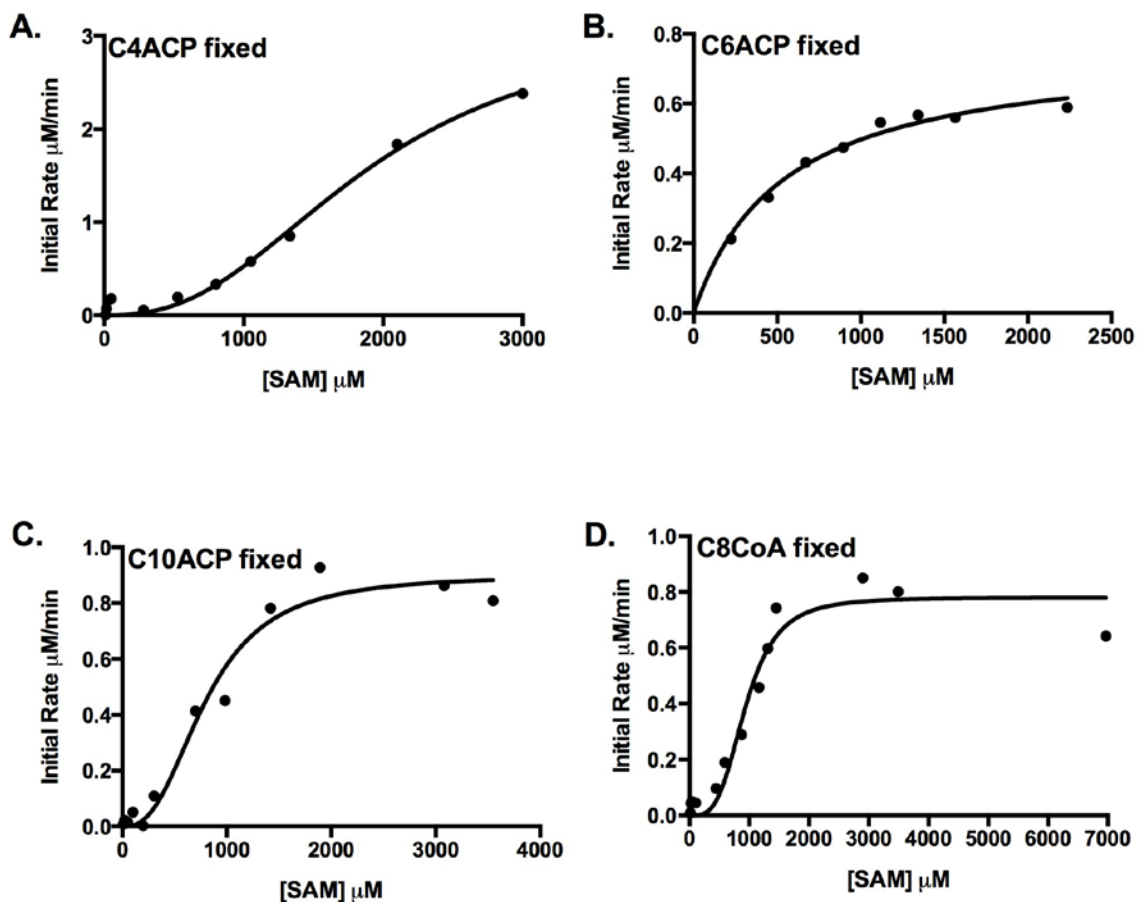
Figure 28.   Substrate-velocity curves for SAM. A-D) Rate curves for SAM when the fixed substrate was 150 μM C4ACP, 38 μM C6ACP, 36 μM C10ACP, and 522 μM C8CoA, respectively. The enzyme concentrations were varied from 0.5 to 5 μM depending on the acyl-ACP substrate used in the experiment. Substrate-velocity data for C6ACP was fit to Michaelis-Menten equation to determine K_m and k_{cat}. Substrates that produced a nonhyperbolic kinetic response were fit to Hill equation to determine Michaelis constant and catalytic constant.

Table 5 is a compilation of the kinetic parameters measured using these substrates with DCPIP. For each variable acyl-ACP, the K_m are not all comparable. The K_m for

variable concentrations of C8ACP with fixed SAM-Cl is 6 ± 1 μM. C6ACP is only two carbons chains shorter than C8ACP and has the most similar K_m. C10ACP is only two carbon chains longer and C4ACP, which is four carbons chains shorter, have the most drastically increased values of K_m. The data suggests that substrates with different acyl-chain lengths from C8ACP have values of K_m increased and are less active. The k_{cat} decreased for alternative substrates. The k_{cat} of C8ACP is 5.8 ± 0.6 min^{-1}. Similarly to the data described above, C6ACP has the most similar turn over number compared to C8ACP. C10ACP is only two carbon chains longer and C4ACP, which is four carbons chains shorter, have the most drastically decreased values of k_{cat}. This data suggests that substrates with different acyl-chain lengths from C8ACP have values of k_{cat} decreased and are less active. Therefore, this data supports that variation in acyl-chain length for acyl-ACPs decreases the activity of BmaI1.

The relative catalytic efficiency all acyl-ACPs and C8CoA were compared in Table 5. C6ACP is only two carbons shorter than the natural substrate and the relative k_{cat}/K_m is 2.5-fold less. C10ACP is two carbons longer than C8ACP and the relative k_{cat}/K_m is 20-fold less than C8ACP. C4ACP is four carbons shorter than the natural substrate and the relative k_{cat}/K_m is 50-fold less than C8ACP. C8CoA is missing the apo-ACP protein and the relative k_{cat}/K_m is 5000-fold less than C8ACP. This huge decrease in catalytic efficiency for C8CoA indicates that ACP binding is important for substrate recognition and turn over. This data also suggests that the catalytic efficiency is reduced for alternative acyl-ACPs and can be the kinetic parameter determining selectivity.

Table 5.   **Effect of acyl-ACP substrates when SAM is fixed on BmaI1 activity**

Variable S	Fixed S	k_{cat} (min^{-1})	K_m μM	k_{cat}/K_m (μM^{-1})(min^{-1})	k_{cat}/K_m Relative[d]
C8ACP[c]	SAM-Cl	5.8 ± 0.6	6 ± 1	0.96 ± 0.18	1.00
C6ACP[c]	SAM-Cl	1.5 ± 0.1	4 ± 1	0.38 ± 0.10	0.40
C4ACP[c]	SAM-Cl	0.60 ± 0.05	29 ± 2	0.021 ± 0.002	0.02
C10ACP[c]	SAM-Cl	0.90 ± 0.10	19 ± 4	0.047 ± 0.011	0.05
C8CoA	SAM-Cl	0.11 ± 0.01	541 ± 14	0.0002 ± 0.00001	0.0002

[c] apo-ACP precipitated, acyl-ACP unprecipitated

[d] [{k_{cat}/ K_m}/{0.96}]

Table 6 is a compilation of the kinetic parameters measured using fixed substrates (C4ACP, C6ACP, C10ACP, C8CoA) and varying SAM-Cl. For each acyl-ACP, the K_m is comparable. The k_{cat}, however, decreased for alternative substrates compared to C8ACP fixed concentrations with variable concentrations of SAM-Cl. The k_{cat} for fixed concentrations of C8ACP with variable concentrations of SAM-Cl is 5.8 ± 0.6 min^{-1}. The k_{cat} for fixed C6ACP with variable SAM-Cl is the most similar to C8ACP, followed by fixed C10ACP and fixed C4ACP with variable SAM-Cl. The alternative substrates are less active with this observed reduction in k_{cat} for fixed acyl-ACP and variable SAM-Cl.

The relative catalytic efficiency for all fixed acyl-ACPs and C8CoA were compared in Table 6. C6ACP is only two carbons shorter than the natural substrate and the measured k_{cat}/K_m was almost identical to C8ACP. C10ACP is two carbons longer than C8ACP and the relative k_{cat}/K_m is 6.3-fold less than C8ACP. C4ACP is four carbons shorter than the natural substrate and the relative k_{cat}/K_m is 5.6-fold less than C8ACP.

C8CoA is missing the apo-ACP protein and the relative k_{cat}/K_m is 20-fold less than

C8ACP. This data also suggests that the catalytic efficiency is reduced for alternative

acyl-ACPs.

Table 6.   **Effect of SAM when acyl-ACP substrates are fixed on BmaI1 activity**

Variable S	Fixed S	k_{cat} (min^{-1})	K_m mM	k_{cat}/K_m (mM^{-1})(min^{-1})	k_{cat}/K_m Relative[d]
SAM-Cl	C8ACP	5.80 ± 0.60	1.80 ± 0.50	3.22 ± 0.96	1.00
SAM-Cl	C6ACP	1.70 ± 0.10	0.54 ± 0.07	3.17 ± 0.46	0.98
SAM-Cl	C4ACP	1.10 ± 0.20	1.91 ± 0.32	0.58 ± 0.14	0.18
SAM-Cl	C10ACP	0.40 ± 0.03	0.80 ± 0.08	0.50 ± 0.06	0.16
SAM-Cl	C8CoA	0.15 ± 0.01	0.94 ± 0.08	0.16 ± 0.02	0.05

[d] $[\{k_{cat}/K_m\}/\{3.22\}]$

Since structural studies have proposed a binding site for ACP with AHL-

synthases, C8CoA was also tested to determine if activity was affected, since it doesn't

contain the ACP protein. When SAM was fixed, there was a 5000-fold decrease in

catalytic efficiency compared to C8ACP. When C8CoA was fixed, there was a 20-fold

decrease in catalytic activity compared to C8ACP. C8CoA assays have the most drastic

decrease in BmaI1 activity compared to the acyl-ACPs. This implies that binding of the

ACP is essential for optimal activity for BmaI1.

Good Substrates Show Hyperbolic Behavior for Both SAM and acyl-ACP and Poor
Substrates Show Sigmoidal Behavior

Figure 27 and 28 show the Velocity vs. [Substrate] curves generated for variable

acyl-ACPs and C8CoA while SAM is fixed and variable SAM while acyl-ACPs and

C8CoA is fixed. Interestingly, many of these curves are not hyperbolic. Table 5 and 6

lists the substrate curve types generated from specific conditions. The natural substrate to BmaI1, C8ACP shows a hyperbolic curve when assayed with DCPIP. C6ACP and C10ACP also have a hyperbolic curve when assayed with DCPIP. These two substrates are only 2 carbon chains different from the natural substrate. C4ACP is four carbons shorter than C8ACP and this substrate shows a sigmoidal curve when assayed with DCPIP. C8CoA lacks the apo-ACP protein and it too has a sigmoidal curve. Both sigmoidal curves show positive cooperativity. This data indicates that good substrates show hyperbolic behavior while poor substrates show sigmoidal behavior.

Good Substrates Show Substrate Inhibition with Fixed SAM

Figure 27 displays the Velocity vs. [Substrate] curves generated for variable acyl-ACPs and C8CoA while SAM is fixed. Substrate inhibition is observed with the natural substrate to BmaI1, C8ACP as well as with C6ACP. Inhibition is not seen with the other substrates. This postulates that good substrates like C8ACP and C6ACP show inhibition when they are varied with fixed SAM-Cl. The above data can be summarized as follows:

1. Good Substrates Show Hyperbolic Behavior for both SAM and acyl-ACP
2. Poor substrates Show Sigmoidal Behavior
3. Good Substrates Show Inhibition with Fixed SAM

Discussion

One objective of the work described in this thesis was to study BmaI1 substrate preparation effects on activity. Additionally, we explored the effects on BmaI1 activity using acyl-ACPs with variable acyl chain lengths. Studying BmaI1 with these alternative substrates provided insight into the kinetic mechanism and helped to understand how this

enzyme discriminates between specific and nonspecific acyl-ACP substrates.   *The BmaI1 substrate specificity study described is our first step towards understanding how AHL-synthase enzymes synthesize one abundant signal from the abundant acyl-ACPs available to achieve QS.*

Does precipitation and resuspension affect acyl-ACP activity with BmaI1 AHL-synthase?

Apo-ACP is precipitated using TCA and sodium deoxycholate while C8ACP is precipitated using acetone. We were interested to check if precipitation and resuspension of these proteins would affect acyl-ACP activity with BmaI1 AHL-synthase. We found that precipitating apo-ACP and not precipitating C8ACP with acetone gave the most active acyl-ACP substrate. ACP is a dynamic protein that interacts in fatty acid biosynthesis with multiple enzyme domains. These interactions have been shown to cause conformational changes in the ACP structure that are pertinent for successful synthesis of acyl-ACPs.[42] Ribbon structures and crystallography studies have shown that AHL-synthases have a specific position for ACP to bind in the active site (Fig. 8).[38-40] It is not unreasonable to predict that the conformation of ACP changes during this interaction. This suggests a specific conformation of ACP is needed during AHL synthesis using AHL-synthases like BmaI1.   If preparation of apo-ACP itself causes a conformational change in ACP that is not native to the BmaI1 reaction, then the rate of activity could change. Additionally, the preparation of the acyl-ACP could induce a change in structure and result in a change in BmaI1 activity.   The samples that were both precipitated or both not precipitated had lower overall rates, which suggest the structure of ACP was altered from its active conformation during preparation.

Does BmaI1 activity change with different SAM formulations such as SAM-chloride and SAM-tosylate?

AHL-synthase structure studies propose a specific binding site for SAM during catalysis (Fig. 8).[38-40] SAM formulations like SAM-Cl and SAM-tosylate contain anionic salts. These salts may inhibit a chemical or enzymatic step necessary for optimal activity of BmaI1. I sought to determine if the chloride or tosylate salt influenced the activity of BmaI1 when coupled with C8ACP. I found that commercially available formulations of SAM-Cl and SAM-tosylate do not affect K_m or k_{cat} measurements of BmaI1. The catalytic efficiency for SAM-Cl was found to be 3.2 $min^{-1}\mu M$ compared to SAM-tosylate at 6.9 $min^{-1}\mu M$. This suggests that SAM-tosylate would be the better substrate to purchase and use when studying BmaI1. However, the curve generated for SAM-tosylate showed inhibition. This inhibition is due to the tosylate salt and lowers the overall V_{max} observed. Therefore, to avoid complication arising from tosylate inhibition, we preferred to use SAM-Cl to study BmaI1.

How does acyl-ACP substrate activity change with acyl chain length? How does the catalytic efficiency of a shorter or longer chain acyl-ACP substrate compare with native substrate?

BmaI1 utilizes C8ACP and SAM to produce C8HSL. The V-cleft in the active site accommodates the C8 acyl chain of C8ACP. It is not unreasonable to predict that shorter and longer acyl chained acyl-ACPs could also 'fit' in this V cleft (Fig. 8). We were interested in studying the effect of variations in acyl chain length on BmaI1 activity. Except the C6ACP substrate, we found that all alternative acyl-ACPs and C8CoA had an increase in K_m and a decrease in k_{cat} compared to C8ACP. Similar results were observed when the concentration of SAM was fixed with adding variable

concentrations of acyl-ACP, as well as when the concentration of the acyl-ACPs were fixed with adding variable concentrations of SAM-Cl. The true understanding of this drop in activity is understood when comparing catalytic efficiencies (k_{cat}/K_m) for each substrate with respect to C8ACP.

When studying the effects of alternative substrates on BmaI1 activity, it is clear that the catalytic efficiency is decreased compared to C8ACP. The most comparable substrate to C8ACP catalytic efficiency was C6ACP, which was 4-fold less active than C8ACP. C10ACP was the next more comparable substrate with a 20-fold decrease in catalytic efficiency. These two substrates are only 2 carbon chains different from the C8ACP. The next substrate studied was C4ACP, which had a 50-fold decrease in catalytic efficiency compared to C8ACP. C4ACP is four carbon chains shorter than C8ACP.

To appreciate how alternative substrates affect BmaI1 activity, it is important to understand how AHL-synthases interact with acyl-ACP substrates. Unfortunately, there have been no enzyme-substrate crystal structures for BmaI1 to date. It is known that when acyl-ACP interacts with other enzymes, the ACP portion docks to a basic residue patch in the partner enzyme. Then the acyl chain is delivered by means of the pantetheine linker to the partner enzyme's active site using a "switch-blade mechanism." [42,44] Cooperative interactions between the acyl-chain-enzyme and the ACP-enzyme site help lock the acyl-chain into a productive conformation. A nucleophile then attacks the carbonyl center of the acyl chain (much like the SAM amine in AHL-synthase reactions) and the reaction proceeds. The rate of the reaction is dependent on the cooperative interaction and the nucleophilic attack step.

It is known that ACP-enzyme interactions are predominantly electrostatic due to the recognition helix II being negatively charged.[44] AHL-synthases like BmaI1 have residues along alpha-7 and beta-8 that form a positively charged patch on the surface (see Fig. 8 for description of amino acids involved in ACP binding). It is not unreasonable to predict that once the acyl chain has been delivered to BmaI1using the panthetheine linker, then the acyl-chain-BmaI1 and the ACP-BmaI1 complexes will undergo cooperative interactions. These interactions help to position the acyl-chain into a productive conformation for the SAM-amine to attack the carbonyl center of the acyl-ACP at the acylation step. If acyl chain length variations alter the cooperative interactions and/or inhibit nucleophilic attack, then the activity of BmaI1 would decrease.

When studying the effects of alternative substrates on BmaI1 activity, it is clear that the catalytic efficiency is decreased compared to C8ACP. The most comparable substrate to C8ACP catalytic efficiency was C6ACP (Table 5). The hexanoyl side chain in C6ACP is not that different from the octanoyl side chain in C8ACP. Perhaps the catalytic efficiency is comparable because the thioester carbonyl of C6ACP could easily be locked in a productive conformation for SAM amine attack. The decrease in catalytic efficiency for C6ACP can possibly be attributed to the slight increase in time it takes for the acyl chain interaction between enzyme and substrate to successfully lock and allow nucleophilic attack.

C10ACP was the next more comparable substrate to C8ACP (Table 5). The decanoyl side chain in C10ACP is only two carbons longer than the octanoyl side chain in C8ACP. This increase in carbon chain length could possibly make the acyl chain bulge out of the V-cleft. This puckering would restrict the flexibility of the acyl chain of

C10ACP and make it difficult to lock it into position for nucleophilic attack.   This would decrease the rate at which the product is turned over (k_{cat}). The next substrate studied was C4ACP, which had a 50-fold decrease in catalytic efficiency compared to C8ACP. C4ACP is four carbon chains shorter than C8ACP. It may also be that a 4-carbon shorter acyl-chain has higher degree of freedom in the acyl-chain pocket. The increase in acyl-chain flexibility would make it difficult to lock the thioester carbonyl carbon in a productive conformation, conducive for nucleophilic attack by SAM-amine. This would drastically decrease the rate at which the product is turned over (k_{cat}).

The final substrate to study was C8CoA, which was 5000-fold less active than C8ACP when used as the variable substrate (Table 5). This drop in catalytic efficiency suggests the rate of product turnover is negligible compared to C8ACP. C8CoA contains the appropriate amount of carbon chains and the pantetheine linker portion necessary for activity but it lacks the ACP. A substrate without the ACP portion could not electrostatically bind to the positively charged residues in BmaI1. When the substrate lacks ACP, the conformational changes needed to lock the carbonyl center of C8CoA into position for nucleophilic attack is nearly impossible.

<u>Does the kinetic mechanism for BmaI1 change between specific and nonspecific
substrates? If this is true, can we get additional insight on how this enzyme discriminates
between specific and nonspecific acyl-ACP substrate?</u>

We have found that the K_i^A for C8ACP is much less than the K_m of SAM-Cl, which suggest BmaI1 follows an ordered sequential mechanism. We have not done any product inhibition experiments to confirm this mechanism. However, we have found that when SAM-Cl was fixed and acyl-ACP was varied the Velocity versus [Substrate] curves were hyperbolic for C8ACP, C6ACP, and C10ACP and sigmoidal for C4ACP and

C8CoA (Table 5). When acyl-ACPs were maintained at a fixed concentration and SAM-Cl was varied, hyperbolic curves were obtained for C8ACP and C6ACP and sigmoidal for C4ACP, C10ACP, and C8CoA (Table 6).

Hyperbolic curves are generated when enzymes respond linearly to changes in substrate concentrations when the varied substrate concentration is low. Enzymes that do not produce hyperbolic curves are non-cooperative and don't follow Michaelis-Menten kinetics. Sigmoidal curves are generated when enzymes do not respond to changes in substrate concentration when the varied substrate concentration is low. This is indicated, as there is no increase in reaction rate as substrate concentration is increased. Upon reaching a threshold concentration, a small increase in substrate concentration produces large changes in initial rate (inflexion region) until the reaction reaches maximal velocity (V_{max}).

Non-hyperbolic rate curves usually indicate a cooperative enzyme. Cooperativity refers to the observation that binding of the substrate or ligand at one binding site affects the affinity of other sites for their substrates. Traditionally, cooperativity required the participation of multiple, spatially distinct binding sites that communicate with ligand-induced structural rearrangements and/or multimeric enzymes.[48] However, studies have shown that cooperativity can occur in the absence of multiple binding sites and without macromolecular oligomerization.[48] AHL-synthases like BmaI1 have only been observed to have one distinct active site (V-cleft) and are monomeric.

Cooperativity for monomeric enzymes with single ligand binding sites was first theorized 40 years ago.[48,49,50] Only a small number of these enzymes have been discovered, which includes the human enzyme that is involved in glucose homeostasis,

glucokinase. These monomeric cooperative systems like traditional cooperative systems have been attributed to slow, substrate induced alterations in enzyme structure. These alterations prevent substrate binding from reaching equilibrium on the timescale of catalytic turnover.[48,50] Therefore, the ability for alternative substrates to produce sigmoidal curves requires an understanding of possible enzymatic mechanisms. The data summarized in the results section can fit at least two mechanistic possibilities.

The Random Sequential Model

The first possible mechanistic model for bisubstrate enzymes is a random sequential mechanism with one pathway more favored than the other (Fig. 29). This model requires that the enzymatic reaction be capable of proceeding through a random ordered mechanism. This model doesn't rely on enzyme conformational heterogeneity or slow interconversion rates.[48] This model predicts that cooperativity can be observed when a random sequential kinetic mechanism has a preferred pathway for substrate addition (Fig. 29). The disfavored pathway can be populated but contributes negligibly to the steady-state reaction velocity because its existence provides a mechanism where 'non-productive' intermediate can accumulate.   The enzyme 3-deoxy-D-arabino-heptulosonate-7-phosphate synthetase from *Rhodomicrobium vannielli* functions according to this model.[48]
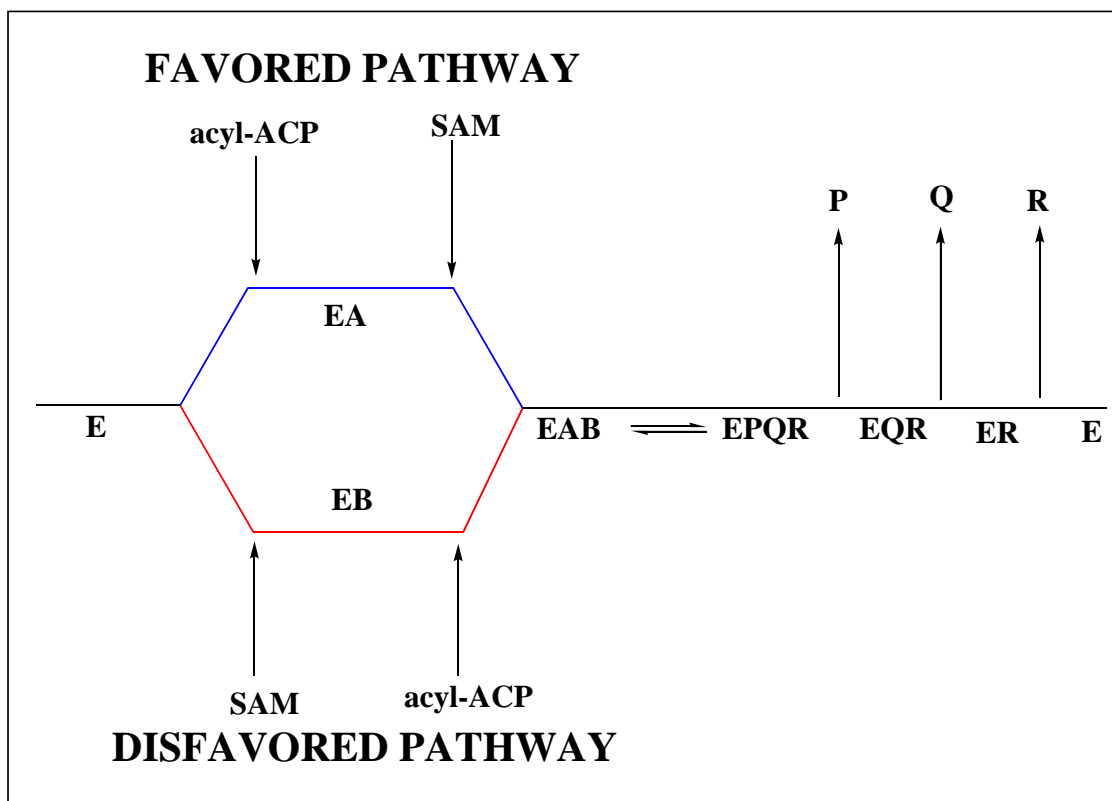
Figure 29. **Random Sequential Mechanism where the Top Pathway is Favored.** The binding of good acyl-ACP substrate follows the top, favored pathway. In this pathway, EA is the BmaI1-acyl-ACP complex. This pathway produces product at a higher rate than the bottom-disfavored pathway where SAM-Cl binds first. In the bottom pathway, EB is the BmaI1.SAM-Cl complex.

The random sequential mechanism where one pathway is favored over the other

can explain the two Velocity versus [Substrate] curve types observed with BmaI1. First,

we can predict the top pathway where acyl-ACP binds to free enzyme E is most

favorable. This is because the K_i^A for C8ACP was significantly less than the K_m for

SAM-Cl. Substrates that produce hyperbolic curves populate the favored pathway. This

could be due to the BmaI1-C8ACP complex (EA) being more stable compared to the

BmaI1.SAM-Cl (EB) complex. The equilibrium favors the formation of EA and thus

increased addition of acyl-ACP substrate show hyperbolic behavior. The EB enzyme

form can convert back to free E and the reaction favorably proceeds with EA form. The

lower pathway does exist, but the more stable EA complex drives the reaction forward via the top pathway.

C8ACP is the native substrate and produces a hyperbolic curve. C8ACP, therefore, populates the favored, more productive pathway and not the 'less-productive/non-productive' pathway because cooperativity isn't observed (Fig. 27). When varying acyl-ACPs, good substrates like C8ACP, C6ACP, and even C10ACP populate the top productive pathway even at low concentrations (Table 5). When SAM-Cl is varied, hyperbolic behavior is observed with C8ACP and C6ACP. For both variable situations, hyperbolic curves result for these substrates because there is not enough free enzyme (E) to form the EB complex. SAM-Cl then binds to the EA form to move the reaction favorably forward.

Poor substrates, like C4ACP and C8CoA (whether fixing SAM or using variable concentrations), cannot populate the top pathway at below threshold concentrations. This could be because these substrates may produce a less stable EA complex and convert back to free E. When SAM is in excess compared to acyl-ACP, free E converts to EB. A significant portion of the enzyme would then exist in the EB form. The EB form is in abundance compared to free enzyme and, so, successive addition of acyl-ACP favors BmaI1.SAM-Cl.acyl-ACP form. This disfavored pathway contributes negligibly to the steady-state reaction velocity and a lag phase in the Velocity versus [Substrate] curve is observed. This pathway can also become abortive with the accumulation of a 'non-productive' complex like BmaI1.SAM-Cl-acyl-ACP. Abortive complexes do not react further to produce product. The rise in the sigmoidal curve occurs when an increase in acyl-ACP concentration drives BmaI1.SAM.acyl-ACP complex back to free enzyme E

(Table 5 and Fig. 27). Since there is an abundance of E, the chances for poor substrates to bind to free enzyme increases. The top pathway will then be populated.

Additional support for this mechanism is seen with the substrate inhibition data (Table 5). The data collected suggests that good substrates show substrate inhibition only when using variable concentrations of acyl-ACPs. This can be attributed to the random sequential model where substrate addition favors one pathway. We discussed that good substrates populate the favored pathway where acyl-ACP binds first followed by SAM-Cl. However, good substrates can also bind to E.SAM complex and form E.SAM.acyl-ACP populating the disfavored pathway, albeit to a smaller extent. Why is substrate inhibition more pronounced beyond saturation? Perhaps, there is too much acyl-ACP substrate around that binds to E.SAM, pushing the reaction more and more towards disfavored pathway. Since this pathway has either a lower turnover rate or is abortive, a decrease in rate is observed. Poor substrates cannot stabilize the EA form until large concentrations are added. Therefore, at low acyl-ACP concentrations, the less favored pathway is populated because most of the enzyme is in E.SAM form. At high concentrations of poor acyl-ACP substrates, the favored pathway is populated. Substrate inhibition is further evidence that the mechanism is random sequential where one pathway is favored and the other is disfavored.

Multiple Free Enzyme Form Model

Sigmoidal curves can result from monomeric enzymes that do not follow the random sequential mechanism with a favored pathway. One such model that attests for monomeric cooperativity is known as the mnemonic model. This model proposes that the conformation of an enzyme following product release can be different from the initial

enzyme state. This requires an oscillation between two enzyme species, a low-affinity conformation (E*) and a high-affinity conformation (E) (Fig. 30A).
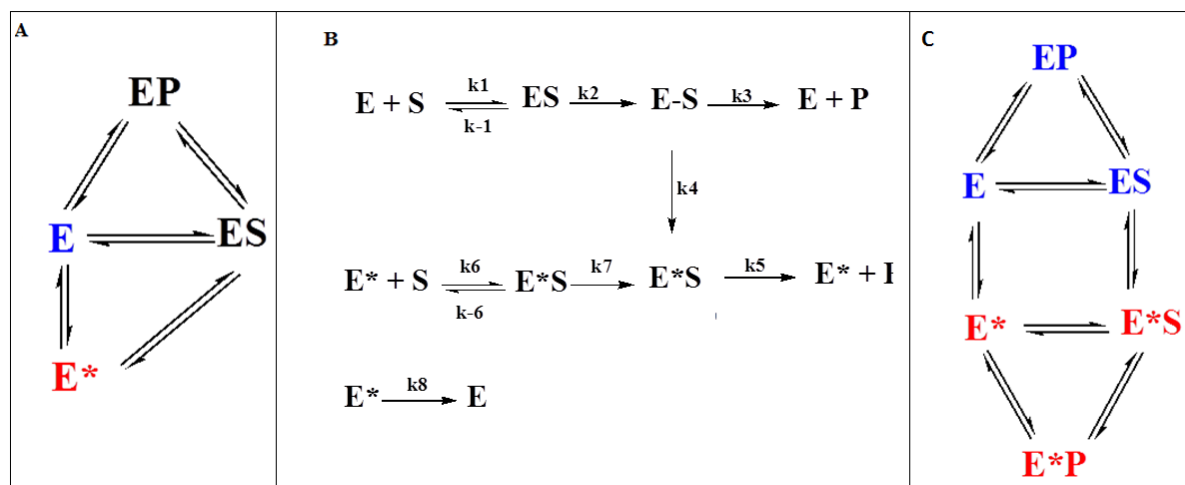
Figure 30.   Multiple Free Enzyme Form Models.   The mnemonic model (A), substrate induced enzyme transition model (B) and the ligand-induced slow transition model (C) require the slow interconversion between two enzyme conformations, a low-affinity (E*) in red and a high-affinity (E) in blue.

For the model to produce positive cooperativity (like observed with our data), the E* species dominates in the absence of substrate. E* to E conversion must be slow. When substrate bind to the less active E* form, conformational transitions occur to release product and to generate the high-affinity enzyme species, E. When substrate is in excess, the high-affinity enzyme form, E, does not have time to 'relax' to the low-affinity form, E*. The enzyme can rapidly bind another molecule of substrate for additional rounds of catalysis. This results in a hyperbolic curve. If substrate is at low concentrations, then E can 'relax' and form E* again. Since E* is the low affinity enzyme form, the curve will look sigmoidal at these low concentrations. [48,50] This model would result in sigmoidal curves for all substrates due to the initially slow transition from E* to E via substrate addition.

An alternative model where substrate addition converts the active enzyme ES complex to a less active E*S complex should also be considered (Fig. 30B; Substrate Induced Enzyme Transition).[51] Both of these forms can convert substrate to product and results in the release of two enzyme forms, E and E*. Additionally, breakdown of the E*S complex generates free enzyme E*. This less active free enzyme form can react with substrate leading to further turnover or spontaneously revert to the more stable enzyme form, E.[51]

An additional model that could describe monomeric cooperativity is known as the Ligand-Induced Slow Transition (LIST) model (Fig. 30C).[48] The LIST model is similar to the mnemonic model in that two enzyme species exists, E* and E. These two species also possess different affinities for substrate. However, the LIST model assumes that without substrate both enzyme forms are in a pre-existing equilibrium. The LIST model also assumes interconversion between these two forms occurs slower than product formation. This prevents equilibration when substrate is associating. This slow step can be due to isomerization or an association-dissociation process. Both conformations are catalytically active, and the steady-state velocity is therefore dependent on the sum of these two catalytic cycle's rates. However, in order to support a multiple free enzyme model, there must be evidence that the enzyme exists in two forms. Structural and pre-steady state kinetics are needed to verify the existence of both enzyme species. Structural studies on acyl-ACP in complex with BmaI1 are in progress.

Both random sequential and multiple free enzyme form models assume the existence of two enzyme forms: the more active E and less active E.* or E.SAM complex. The acyl-ACPs can bind to either form. Considering these models with the data

obtained, the addition of good substrates like C8ACP, C6ACP, and even C10ACP shift

the equilibrium between these two enzymes species to the more active BmaI1 form. The

more active enzyme would have a higher rate of turnover and a hyperbolic curve should

be observed.

Burkart and co-workers observed that when ACP binds to enzymes the acyl chain

is released to the acyl chain pocket in the partner enzyme.[52] Perhaps these poor substrates

with nonspecific acyl chains do not fit well in the acyl chain pocket (V-cleft) of BmaI1.

This lack of fit could revert the chain back to being sequestered into the ACP, which

could make BmaI1.acyl-ACP complex less stable. In addition, for nonspecific substrates,

the Enzyme.acyl-ACP complex may also be less productive. Therefore, a nonspecific

acyl-ACP substrate could result in a less stable and less productive BmaI1.acyl-ACP

complex thereby keeping the AHL-synthase rates low compared to the native acyl-ACP

substrate. Our results also suggest that both binding and catalytic steps are affected when

a nonspecific acyl-ACP substrate binds to BmaI1 AHL synthase. It is now clear that

native acyl-ACP substrate recognition occurs at more than one step during AHL

synthesis.

Conclusion

This thesis work is the first study to report differences in rates and mechanism for
nonspecific acyl-ACP substrate reacting with an AHL-synthase.

When studying BmaI1, we observed that the method of preparation of apo-ACP

and the acyl-ACP is important to achieve optimum activity. SAM-Cl and SAM-tosylate

do not affect BmaI1 optimum activity. Therefore, either substrate can be used to study

AHL synthase. We found that catalytic efficiency for nonspecific acyl-ACP substrate is

drastically low compared to C8ACP. *This decrease in activity explains tight signal specificity in bacterial QS, in vivo.* The kinetic mechanism suggests a random sequential mechanism where one pathway (acyl-ACP binding first to the free enzyme) is favored over the other pathway (SAM binding first to the free enzyme). Our data suggest that acyl-ACP substrate can bind to at least two enzyme forms. The formation of a stable and productive E.acyl-ACP complex is critical in AHL synthesis. Based on our data with alternative substrates, we infer that the E.acyl-ACP complex is less stable and less productive for nonspecific acyl-ACP substrates. Finally, acyl-ACP substrate recognition occurs at multiple steps in AHL synthesis.

REFERENCES

1. Fuqua, C., and Greenberg, E. P. "Listening in on bacteria: acyl-homoserine lactone signaling." *Nat. Rev. Mol. Cell Biol.* (**2002**), *3,* 685-695.

2. Bonnie L. Bassler, "Small Talk: Cell –to-cell communication in Bacteria." *Cell* (**2002**)*,* *109*, 421-424.

3. Miller, M. B.; Bassler, B. L. "Quorum Sensing in Bacteria." *Annu. Rev. Microbiol.* (**2001**), *55,* 165-199.

4. Finch, R.G.; Pritchard, D.I.; Bycoft, B.W.; William, P.; Steward, G.S.A. "Quorum Sensing: a novel target for anti-infective therapy." *J. Antimicrob. Chemother.* (**1998**), *42,* 569-571.

5. Defoirdt, T.; Boon, N.; Bossier, P. "Can Bacterial Evolve Resistance to Quorum Sensing Disruption." *PLoS Pathog.* (**2010**), *6,* 1-6.

6. Rutherford, S. T.; Bassler, B. L. W. A. "Bacterial Quorum Sensing: Its Role in Virulence and Possibilities for Its Control." *Cold Spring Harbor Perspect Med.* (**2012**), *2,* 1-25.

7. LaSarre, B.; Federle, M. J. "Exploiting Quorum Sensing To Confuse Bacterial Pathogens." *Microbiol Mol Rev.* (**2013**)*, 77,* 73-111.

8. George, E. A.; Muir, T. W. "Molecular Mechanisms of agr Quorum Sensing in Virulent Staphylococci." *Chem. Bio. Chem.* (**2007**), *8,* 847-855.

9. Bassler, B. L. "How bacteria talk to each other: regulation of gene experession by quorum sensing." *Curr. Opin. Micro-bio.* (**1999**), *2, 582-587.*

10. De Keive T.R., Iglewski, B.H. "Bacterial quorum sensing in pathogenic relationships." *Infect. Immun.* (**2000**), *68*, 4839-49.

11. Fuqua C.; Winanas S.C.; Greenberg, E. P. "Census and consensus in bacterial ecosystems: the LuxR-LuxI family of quorum-sensing transcriptional regulators." *Annu. Rev. Microbiol.* (**1996**), 50:727-51.

12. Parsek, M.R.; Greenberg, E.P. "Acylhomoserine lactone quorum sensing in gram-negative bacteria: a signaling mechanism involved in associations with higher organisms." *Proc. Natl. Acad. Sci.* (**2000**) USA, *97*, 8789-93.

13. Raychaudhuri, A.; Tullock, A.; Tipton, P. A. "Reactivity and Reaction Order in Acylhomoserine Lactone Formation by Pseudomonas Aeruginosa RhlI." *Biochemistry* (**2008**)*, 47,* 2893-2898.

14. Schuster, M., Lostroh, C.P., Ogi, T., and Greenberg, E. P. "Identification, timing, and signal specificity of *Psuedomonas aeruginosa* quorum-controlled genes; a transcriptome analysis." *J. Bacteriol.* (**2003**), *185,* 2066-2079.

15. Wagner, V. E., Bushnell, D., Passador, L., Brooks, A. I., and Iglewski, B. H. "Microarray analysis of *Pseudomonas aeruginosa* quorum-sensing regulons: effects of growth phase and environment." *J. Bacteriol.* (**2003**), *185,* 2080-2095.

16. Pereira, C. S.; Thompson, J. A.; Xavier, K. B. "AI-2-Mediated Signaling in Bacteria." *FEMS Microbiol. Rev.* (**2013**), *37,* 156-181.

17. Singh, A.; Del Poeta, M. "Lipid signaling in Pathogenic Fungi." *Cell Microbiol.* (**2011**), *13,* 177-185.

18. Chen, X.; Schauder, S.; Potier, N.; Van Dorsselaer, A.; Pelczer, I.; Bassler, B. L.; Hughson, F. M. "Structural Identification of a Bacterial Quorum-Sensing Signal Containing Boron." *Nature* (**2002**), *415,* 545-549.

19. Hardie, K. R.; Heurlier, K. "Establishing Bacterial Communities by 'Word of Mouth': LuxS and Autoinducer 2 in Biofilm Development." *Nat. Rev. Microbiol.* (**2008**), *6,* 635-643.

20. Kolter, R.; Greenberg, E. P. "The Superficial Life of a Microbes." *Nature* (**2006**), *441,* 300-302.

21. Watnick, P.; Kolter, P. "Biofilm, City of Microbes." *J. Bacteriol.* (**2000**), *182,* 2675-2679.

22. Davies, D. "Understanding Biofilm Resistance to Antibacterial Agents." *Nat. Rev. Drug Discov.* (**2003**)*, 2,* 114-122.

23. Antunes, L. C.; Ferreira, R. B.; Buckner, M. M.; Finlay, B. B. "Quorum Sensing in Bacterial Virulence." *Microbiology* (**2010**), *156,* 2271-2282.

24. Fleming, A. "On the Antibacterial Action of Cultures of a *Penicillium,* with Special Reference to Their Use In the Isolation of *B. influenza*." *Brit. J. of Exp. Path.* (**1929**), *10,* 226-236

25. Abraham, E.P. "Chain, E., An Enzyme from Bacteria Able to Destroy Penicillin." Rev. Infect. Dis. (**1940**), *10,*677-678.

26. Ni, N.; Li, M.; Wang, J.; Wang, B. "Inhibitors and Antagonists of Bacterial Quorum Sensing." *Med Res Rev.* (**2008**), *29,* 65-124.

27. Geske, G. D.; Wezeman, R. J.; Siegel, A. P.; Blackwell, H. E. "Small Molecule Inhibitors of Bacterial Quorum Sensing and Biofilm Formation." *J Amer Chem Soc.* (**2005***), 127,* 12762-12763.

28. Borlee, B.R. "Identification of synthetic inducers and inhibitors of the quorum-sensing regulator LasR in *Pseudomonas aeruginosa* by high-throughput screening." *Appl. Environ. Microbiol.* (**2010**), *76*, 8255.

29. Geske, G.D.; O'Neill, J.C.; Miller, D.M.; Wezeman, R.J.; Mattmann, M.E.; Lin, Q.; Blackwell, H.E. "Comparative Analyses of N-Acylated Homoserine Lactones

Reveal Unique Structural Features that Dictate Their Ability to Activate or Inhibit Quorum Sensing." *Chem BioChem* **(2008)**, *9,* 389-400.

30. Pearson, J.P.; Feldman, M.; Iglewiski, B.H.; Prince, A. "*Pseudomonas aeruginosa* Cell-to-Cell Signaling Required for Virulence in a Model of Acute Pulmonary Infection." *Infect. Immun.* **(2000)**, *68,* 4331-4334.

31. Jeddeloh, J.A.; Oyston, P., Ulrich, R. Glanders/meliodosis Vaccines. W02004006857 A2, Jan. 22, 2004.

32. Duerkop, B.A. "Octanoyl-homoserine lactone is the cognate signal for Burkholderia mallei BmaR1-BmaI1 quorum sensing." J. Bacteriol. **(2007)**, *189*, 5034.

33. Duerkop, B.A. "The Burkholderia mallei BmaR3-BmaI3 quorum-sensing system produces and responds to N-3-hydroxy-octanoyl homoserine lactone." J. Bacteriol. **(2008)**, *190*, 5137.

34. Desiderio, C.; Cavallaro, R.A., De Rossi, A., D'Anselmi, F., Fuso, A., and Scarpa, S. "Evaluation of chemical and diasterisomeric stability of S-adenosylmethionine in aqueous solution by capillary electrophoresis." *J. Pharm. Biomed. Anal.* **(2005)**, *38,* 449-456.

35. Rock, C.O.; Garwin, J.L.; Cronan, J.E. "Preparative enzymatic synthesis of acyl-acyl carrier protein" *Methods Enzymol.* **(1981)**, *72*, 397-403.

36. Parsek, M. R.; Schaefer, A. L.; Greenberg, E. P. "Analysis of random and site-directed mutation in RhlI, a *Pseudomonas aeruginosa* gene enconding an acylhomserine lactone synthase." *Mol. Microbiol.* **(1997)**, *26,* 301-310.

37. Christensen, Q.H.; Grove, T.L.; Booker, S.J.; Greenberg, P.E. "A High-throughput Screening for Quorum-Sensing Inhibitors that Target acyl-homoserine lactone Synthases." *PNAS,* **(2013)**, *110,* pg.13815.

38. Gould, T.A.; Schweizer, H. P.; Churchill, M. E.A. "Structure of Pseudomonas aeruginosa acyl-homoserinelactone synthase." *Molecular Microbiology* **(2004)**, *53,* 1135-1146.

39. Watson, W. T.; Minogue, T.D.; Val, D. L.; Von Bodman, S. B.; Churchill, M.E.A. "Structural basis and specificity of acyl-homoserine lactone signal production in bacterial quorum sensing." *Mol. Cell* **(2002)**, *9,* 685-694.

40. Watson, W.T. "Crystallization and rhenium MAD phasing of the acyl-homoserinelactone synthase EsaI." Acta crystallographica. Section D, Biological crystallography **(2001)**, *57*, p. 1945.

41. Chan, D. I.; Stockner, T.; Tieleman, D. P.; Vogel, H. J. "Molecualr Dynamics Simulations of the Apo-, Holo-, and Acl-forms of Escherichia Coli Acyl Carrier Protein." **(2008)***, 283,* 33620-33629.

42. Rafi, S.; Novichenok, P.; Kolappan, S.; Zhang, X.; Stratton, C. F.; Rawat, R.; Kisker, C.; Simmerling, C.; Tonge, P. J. "Structure of Acyl Carrier Protein Bound to Fabl, The FasII Enoyl Reductase from Escherichia Coli." *J. Biol. Chem.* **(2006)***, 281,* 39285-39293.

43. Hoang, T. T.; Sullivan, S. A.; Cusick, J.K.; Schweizer, H. P. "Beta-Ketoacyl acyl carrier protein reductase (FabG) activity of the fatty acid biosynthetic pathway is a determining factor of 3-oxo-homoserine lactone acyl chain lengths." *Microbiology*, **(2002)**, *148,* 3849-3856.

44. Gong, H.; Murhy, A.; Mcmaster, C. R.; Byers, D. M. "Neutralization of Acidic Residues in Helix II Stabilized the Folded Conformation of Acyl Carrier Protein and Variably Alters Its Function with Different Enzymes." *J. Biol. Chem.* **(2006)**, *282,* 4495-4503.

45. Gould, T. A.; Herman, J.; Krank, J.; Murphy, R.C.; Churchill, M.E.A. "Specificity of Acyl-Homoserine lactone synthases examined by mass spectrometry." *J. Bacteriol.* **(2005)**, *188,* 773-783.

46. Raychaudhuri, A.; Jerga, A.; Tipton, P. A. "Chemical Mechanism and Substrate Specificity of RhlI, an Acylhomoserine Lactone Synthase from Pseudomonas Aeruginosa." *Biochemistry* **(2005)**, *44,* 2974-2981.

47. Experiment conducted by Ryan Brecht in Nagarajan Lab.

48. Porter, C.M.; Brian, G.M. "Cooperativity in monomeric enzymes with single linand-binding sites." *Bioorganic Chemistry,* **(2012)**, *43,* 44-50.

49. B.R. Rabin. "Co-operative effects in enzyme catalysis: a possible kinetic model based on substrate-induced conformation isomerization." *Biochem. J.* **(1967)**, *102,* 22c-23c.

50. Storer, A.C. Cornish-Bowden, A. "Kinetic Evidence for a "Mnemonical" Mechanism for Rat Liver Glucokinase." *Biochem, J.* **(1977)**, *165,* 61-69.

51. Kumar, S.; Adediran, A; Nukaga, M.; Pratt, R.F. "Kinetics of Turnover of Cefotaxime by the *Enterobacter cloace* P99 and GCl β-Lactamasese: Two Free Enzyme Forms of the P99 β-Lactamases Detected by a Combination of Pre- and Post-Steady State Kinetics." *Biochemistry*, **(2004)**, *43*, 2664-2672.

52. Burkart, M. "ACP modification to understand protein-protein interactions in fatty acid biosynthesis." *The FASEB Journal,* **(2014)**¸*28.*